Experimental and Theoretical Studies of the Mechanism and Thermochemistry of Formation of α,n-Dehydrotoluene Biradicals from Gas-Phase Halide Elimination Reactions†

Paul G. Wenthold, Scott G. Wierschke, John J. Nash, and Robert R. Squires*

Contribution from the Department of Chemistry, Purdue University, West Lafayette, Indiana 47907

Received January 21, 1994. Revised Manuscript Received May 6, 1994®

Abstract: Absolute heats of formation for α,2-, α,3-, and α,4-dehydrotoluene biradicals have been determined from the measured threshold energies for dissociation of chloride, bromide, and iodide ion from the corresponding *o*-, *m*-, and *p*-halobenzyl anions in the gas phase. The apparent heats of formation derived for the α,2- and α,4-dehydrotoluene biradicals exhibit a dependence upon the particular halide ion used for the threshold energy measurement (decreasing with increasing halide atomic number), while the final heat of formation obtained for the α,3-dehydrotoluene biradical is invariant with changes in the halide. The 298 K heats of formation derived from the iodobenzyl anion results for α,2-, α,3-, and α,4-dehydrotoluene are all found to be 103 ± 3 kcal/mol. This value is in fair agreement with the predicted heats of formation for the ground state of each biradical obtained from MCSCF calculations (105–106 kcal/mol) and significantly lower than the value of 107.6 ± 1.7 kcal/mol predicted by a simple bond energy additivity calculation. The MCSCF calculations indicate α,2- and α,4-dehydrotoluene to be ground-state triplet biradicals with open-shell singlets lying 7.4 and 8.1 kcal/mol higher in energy, respectively, while α,3-dehydrotoluene is found to be a ground-state singlet with the triplet lying 3.0 kcal/mol higher in energy. The halide ion dependence of the apparent heats of formation for the α,2- and α,4-dehydrotoluene biradicals is attributed to the spin-forbidden nature of the dissociation reactions that produce them. The intersystem crossing required to form ground-state triplet products from the halobenzyl anion precursors is associated with a reverse activation energy and/or a kinetic shift in the reaction onset due to slow unimolecular decomposition kinetics. Both effects would be expected to diminish with the heavier halides. In contrast, dissociation of a *m*-halobenzyl anion to produce α,3-dehydrotoluene is spin-allowed, so the reaction occurs at the true thermochemical limit.

We have been developing the use of collision-induced dissociation (CID) threshold energy measurements as a means to determine absolute heats of formation for carbenes[1] and biradicals.[2] The method involves the determination of an accurate translational energy threshold for collisionally-activated halide elimination from either an α-halocarbanion (for carbenes) or an α,ω-halocarbanion (for biradicals). The measured activation energy for halide loss is then combined with auxiliary thermochemical data for the reactant and product ions according to a simple thermochemical cycle to derive the heat of formation of the neutral product. This approach has been successfully applied to the determination of heats of formation for CCl_2,[1b] CF_2,[1b] and other chlorofluorocarbenes,[1a,c] as well as for *o*-, *m*-, and *p*-benzyne.[2] A common feature of these earlier experiments is that the neutral fragments are all ground-state singlets with either σ^2 or $\sigma^1\sigma^1$ electronic configurations for which the halide elimination reactions that produce them are both spin- and symmetry-allowed. This is an ideal situation for deriving thermochemistry from CID threshold measurements since the dissociation reactions can occur on a single potential energy surface without complications due to a reverse activation energy.

In a preliminary report,[3] we recently described an application of the CID threshold technique to the α,n-dehydrotoluene biradicals **1**, **2**, and **3** (Scheme 1). These dissociation reactions

Scheme 1

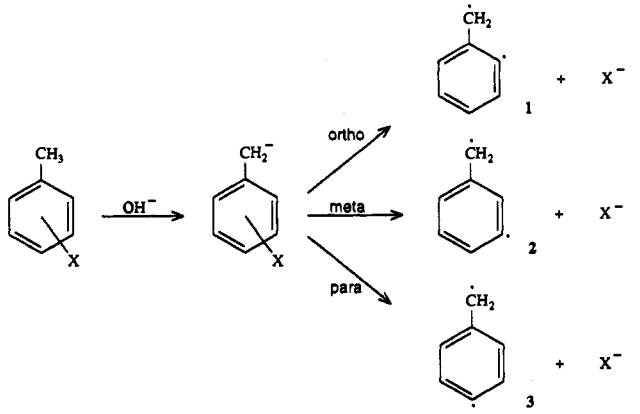

are qualitatively quite different from those examined earlier. Because the α,n-dehydrotoluenes are σ,π-biradicals with one unpaired electron in the benzylic π-orbital and one in a phenyl σ-orbital, their formation by dissociation of a halide ion from *o*-, *m*-, and *p*-halobenzyl anions is formally symmetry-forbidden for mechanisms involving in-plane departure of the halide ion leaving group.[4] In addition, α,2-dehydrotoluene (**1**) is known to be a ground-state triplet ($^3A''$),[5] and α,4-dehydrotoluene (**3**) is reasonably expected to be a ground-state triplet ($^3B_1$) based on its similarity to **1** and to α,4-dehydrophenol, another known triplet-

† Biradical Thermochemistry from Collision-Induced Dissociation Threshold Energy Measurements. Part 2. For part 1, see Wenthold, P. G.; Squires, R. R. *J. Am. Chem. Soc.* **1994**, *116*, 6961.

* Abstract published in *Advance ACS Abstracts*, July 1, 1994.

(1) (a) Paulino, J. A.; Squires, R. R. *J. Am. Chem. Soc.* **1991**, *113*, 1845. (b) Paulino, J. A.; Squires, R. R. *J. Am. Chem. Soc.* **1991**, *113*, 5573. (c) Paulino, J. A. Ph.D Thesis, Purdue University, 1992.

(2) (a) Wenthold, P. G.; Paulino, J. A.; Squires, R. R. *J. Am. Chem. Soc.* **1991**, *113*, 7414. (b) Wenthold, P. G.; Squires, R. R. *J. Am. Chem. Soc.* **1994**, *116*, 6961.

(3) Wenthold, P. G.; Wierschke, S. G.; Nash, J. J.; Squires, R. R. *J. Am. Chem. Soc.* **1993**, *115*, 12611.

(4) (a) Turro, N. J. *Modern Molecular Photochemistry*, Benjamin/Cummings Publ. Co.: Menlo Park, CA, 1978; Chapter 7. (b) Michl, J. In *Chemical Reactivity and Reaction Paths*; Klopman, G., Ed.; J. Wiley and Sons: New York, NY, 1974; Chapter 8.

(5) Closs, G. L.; Kaplan, L. R.; Bendall, V. I *J. Am. Chem. Soc.* **1967**, *89*, 3376.

0002-7863/94/1516-7378$04.50/0

state biradical.[6] In our preliminary report on these species, we described the results of MCSCF calculations on their structures, energies, and singlet–triplet splittings.[3] The calculations not only verified the triplet ground-state assignments for **1** and **3** but also showed that α,3-dehydrotoluene (**2**) is a ground-state *singlet* biradical with the triplet state lying *ca.* 3.0 kcal/mol higher in energy. This prediction is consistent with the documented reactivity of **2** in solution[7] and with the observed CID behavior of *m*-halobenzyl anions reported in the earlier study.[3] Therefore, with these variable symmetry and spin aspects, halide eliminations from *o*-, *m*-, and *p*-halobenzyl anions represent potentially complex dissociations that may involve one or more curve-crossings. Such behavior could give rise to reverse activation energies and/or kinetic shifts, thereby compromising the utility of these reactions for deriving thermochemical data.

In this paper we present the full details of the CID threshold energy measurements, data analysis, and theoretical studies involving the α,n-dehydrotoluene biradicals, along with a discussion of the mechanistic and dynamical features of halobenzyl anion dissociation reactions. A consistent set of absolute heats of formation for the three biradicals is derived that is in satisfactory agreement with the theoretical calculations. The measured and calculated energetics for the α,n-dehydrotoluene biradicals reveal a previously unrecognized stabilization relative to simple models based on bond energy additivity. Finally, using the measured heats of formation for **1**, **2**, and **3**, we derive additional thermochemical data such as the energy of cycloaromatization of (*Z*)-1,2,4-heptatrien-6-yne and the ring C–H bond strengths in benzyl radical.

Experimental Section

All experiments were carried out with a flowing afterglow–triple quadrupole apparatus that is described in detail elsewhere.[8,9] The standard operating conditions used for these experiments were $P(He)$ = 0.4 Torr, flow(He) = 200 STP cm³/s and velocity(He) = 9400 cm/s. Primary reactant ions are formed by electron ionization of pure gases added near an electron emission source located at the upstream end of the flow tube. Hydroxide ion was generated by ionization of a mixture of N_2O and CH_4, and fluoride ion was formed by ionization of NF_3. The ions are carried through a 100-cm × 7.3-cm i.d. flow reactor by the helium buffer gas and are allowed to react with neutral reagent gases added through regularly-spaced inlet valves. *o*-, *m*-, and *p*-halobenzyl anions were prepared by proton abstraction from the corresponding *o*-, *m*-, or *p*-halotoluene by hydroxide ion. Other anion bases used for the acid–base bracketing experiments were prepared by deprotonation of the neutral conjugate acid by either OH^- or F^-.

Ions generated in the flow tube are thermalized to ambient temperature (*ca.* 298 K) by up to 10^5 collisions with the helium buffer gas prior to sampling. Ions of the selected charge type are gently extracted from the flow tube through a small orifice in a nose cone and then focused into an EXTREL triple quadrupole mass analyzer. For collision-induced dissociation studies, the ion of interest is selected with the first quadrupole (Q1) and then injected with variable kinetic energy into the second quadrupole (Q2; rf only), which serves as a gas-tight collision chamber. Neon and argon were used as collision gases for the CID experiments in this study. The gas pressure in the collision region is kept below 5×10^{-5} Torr in order to minimize secondary ion–target collisions. The ion axial kinetic energy in Q2 is determined by the quadrupole rod offset voltage, which can be varied over a range of 0–200 V. Reactant and product ions are mass-selected with the third quadrupole (Q3) and then detected with an electron multiplier operated in pulse counting mode.

Collision-Induced Dissociation Threshold Energy Measurements. The data collection and analysis procedures used for CID threshold measurements with the flowing afterglow, triple quadrupole apparatus have been described in detail previously.[1,10,11] For these experiments, the product ion yield or partial cross section for CID of the mass-selected reactant ion is monitored while the Q2 rod offset voltage is scanned. The ion/target collision energy in the center-of-mass frame (E_{CM}) is given by $E_{CM} = E_{lab}[m/(M+m)]$, where E_{lab} is the nominal lab energy, M is the mass of the reactant ion, and m is the mass of the neutral target. The target masses used in this study were 20.2 amu for neon and 40 amu for argon. The ion kinetic energy origin and beam energy spread were determined by retarding potential analysis, with Q2 serving as the retarding field element. The ion beam energy distributions are approximately Gaussian in shape, with a typical full-width at half-height of 0.5–1.5 eV (lab frame). The uncertainty in the beam energy origin is approximately 0.1 eV (lab frame).

Absolute cross sections for formation of a single product from CID (σ_p) are calculated using $\sigma_p = I_p/INl$, where I_p and I are the intensities of the product and reactant ions, respectively, N is the number density of the target gas, and l is the effective collision path length. This relationship is valid as long as the target number density is kept sufficiently low that the total extent of dissociation is less than *ca.* 5%, i.e., in the thin-target limit. The effective path length in the collision cell is measured to be 24 ± 4 cm based on calibration experiments with the reaction $Ar^+ + D_2 \rightarrow ArD^+ + D$, which has a well-established cross section.[12] The reported absolute cross sections are the averages of replicate measurements and have estimated uncertainties of ±50%. Relative cross sections are more accurate, with estimated uncertainties of ±20%.

A plot of the CID cross section versus E_{CM} gives an ion appearance curve from which the dissociation energy can be derived. The data are fit with a model threshold law that is convoluted with certain distribution functions that can cause broadening of the dissociation onset. In addition, in order to account for the potential effects of kinetic shifts in the dissociation onset that can result from slow unimolecular decomposition, the model includes dissociation probability factors obtained from RRKM analysis. The composite model function is given in eq 1, where $\sigma(E)$ is the cross section at energy E, E_T is the threshold energy, σ_0 was a scaling factor, and n is an adjustable parameter.[13] The index i denotes reactant

$$\sigma(E) = \sigma_0 \sum_i [g_i P_D(E,E_i,\tau)(E + E_i - E_T)^n/E] \qquad (1)$$

ion vibrational states having energy E_i and population g_i ($\Sigma g_i = 1$), and P_D is the probability that metastable ions formed with initial translational energy E and internal energy E_i will dissociate within the experimental time window, τ (*ca.* 30 μs, the estimated flight time from Q2 to Q3 of an activated ion in a "typical" CID reaction[9]). This model for CID cross sections is essentially the same as that developed by Armentrout and co-workers,[14] except for the omission of a term for the effects of rotational energy since we assume that it is conserved in CID reactions. The internal energy distributions of the reactant ions were estimated from calculated vibrational frequencies obtained from semiempirical molecular orbital calculations using the MOPAC 6.0 package and the AM1 Hamiltonian.[15] The computed harmonic frequencies determined for each of the geometry-optimized species were scaled by a factor of 0.9. The dissociation probabilities, P_D, were obtained by calculating the unimolecular decay rate as a function of reactant ion internal energy in accordance with the RRKM method.[16] For this analysis, the density of states for the reactant ions was obtained from the scaled molecular vibrational frequencies. For the dissociation transition states, the frequencies computed for each separate product biradical were combined with two 25-cm⁻¹ frequencies to represent the two nondegenerate carbon–halide bending modes (*vide infra*).

(6) (a) Arnold, B. R.; Scaiano, J. C.; Bucher, G. F.; Sander, W. *J. Org. Chem.* **1992**, *57*, 6469. (b) Sander, W.; Müller, W.; Sustmann, R. *Angew. Chem., Int. Ed. Engl.* **1988**, *27*, 572.

(7) Myers, A. G.; Dragovich, P. S.; Kuo, E. Y. *J. Am. Chem. Soc.* **1992**, *114*, 9369.

(8) Graul, S. T.; Squires, R. R. *Mass Spectrom. Rev.* **1988**, *7*, 1.

(9) Marinelli, P. J.; Paulino, J. A.; Sunderlin, L. S.; Wenthold, P. G.; Poutsma, J. C.; Squires, R. R. *Int. J. Mass. Spectrom. Ion Processes* **1994**, *130*, 89.

(10) Sunderlin, L. S.; Wang, D.; Squires, R. R. *J. Am. Chem. Soc.* **1992**, *114*, 2788.

(11) Sunderlin, L. S.; Wang, D.; Squires, R. R. *J. Am. Chem. Soc.* **1993**, *115*, 12060.

(12) Ervin, K. M.; Armentrout, P. B. *J. Chem. Phys.* **1985**, *83*, 166.

(13) (a) Chesnavich, W. J.; Bowers, M. T. *J. Phys. Chem.* **1985**, *83*, 900. (b) Sunderlin, L. S.; Armentrout, P. B. *Int. J. Mass Spectrom. Ion Processes* **1989**, *94*, 149 and references therein.

(14) (a) Schultz, R. H.; Crellin, K. C.; Armentrout, P. B. *J. Am. Chem. Soc.* **1991**, *113*, 8590. (b) Khan, F. A.; Clemmer, D. E.; Schultz, R. H.; Armentrout, P. B. *J. Phys. Chem.* **1993**, *97*, 7978.

(15) AM1: Dewar, M. J. S.; Zoebisch, E. G.; Healy, E. F.; Stewart, J. J. P. *J. Am. Chem. Soc.* **1985**, *107*, 3902. MOPAC: Stewart, J. J. P. *QCPE* No. 455.

(16) (a) Robinson, J. P.; Holbrook, K. A. *Unimolecular Reactions*; Wiley-Interscience: New York, 1972. (b) Forst, W. *Theory of Unimolecular Reactions*; Academic: New York, 1973.

Analysis of the experimental data using eq 1 is carried out by an iterative procedure in which σ_0, n, and E_T are varied so as to minimize the deviation between the steeply rising portions of the calculated and experimental appearance curves.[17] As in all our previous CID work, the region near the reaction onset is not included in the fit due to tailing in the data that is attributed to fragmentation caused by collisional activation of the reactant ion outside of the nominal collision region.[9,11] Convoluted with the trial excitation function are the reactant ion kinetic energy distribution, approximated by a Gaussian function with a 1.5-eV width, and a Doppler broadening function developed by Chantry[18] to account for random thermal motion of the neutral target. Because of the explicit inclusion of the reactant ion thermal energy content in the fitting procedure, the CID threshold energy obtained in this way corresponds to the 0 K dissociation energy, i.e., ΔE_0. The corresponding ΔE_{298} values are obtained by adding the difference in integrated heat capacities for the products and reactants (also obtained from semiempirical MO calculations[15]). For deriving heats of formation, an additional factor of RT (0.59 kcal/mol at 298 K), corresponding to the PV work term for dissociation, is also added to convert ΔE_{298} to an enthalpy change.

Materials. Gas purities were as follows: He (99.995%), Ar (99.955%), Ne (99.999%), N_2O (99%), CH_4 (99%), and NF_3 (98%). All reagents were obtained from commercial vendors and used as supplied except for degassing of liquid samples prior to use.

Computational Details. Optimized geometries for the triplet and open-shell singlet states of **1**, **2**, and **3** were obtained with C_s, C_s, and C_{2v} symmetry constraints, respectively, using an MCSCF procedure with two different active orbital spaces. The smaller of these, MCSCF(2,2), has two active electrons in the two nonbonding σ- and π-orbitals. The larger active space, MCSCF(8,8), has eight active electrons distributed among all symmetry-allowed configurations involving the nonbonding σ-orbital, the nonbonding π-orbital (π_4), and the six π- and π^*-orbitals (π_1–π_3 and π_5–π_7, respectively). The 3-21G basis set[19] was used for the larger active space geometry optimizations, and the 6-31G* basis set[19] including six d-functions on the carbon atoms was employed for the MCSCF(2,2) optimizations. Geometry optimizations for the closed-shell singlet states of **1** (C_s), **2** (C_1), and **3** (C_{2v}) were carried out using analogous MCSCF(2,2)/6-31G* procedures for **1** and **3** and an RHF/6-31G* procedure for **2**. Optimized geometries for benzene (D_{6h}),[20] phenyl radical (C_{2v}),[20] and benzyl radical (C_{2v}) were obtained at the MCSCF(6,6), MCSCF(7,7), and MCSCF(7,7) levels, respectively, with the 3-21G basis set. The active spaces in these calculations are analogous to the larger active spaces used for **1**, **2**, and **3**, allowing correlation between all π- and π^*-orbitals and, in the case of phenyl radical, the non-bonding σ orbital. Harmonic vibrational frequencies were obtained for **1**–**3** at the MCSCF(2,2)/6-31G* level, for ^{1}A **2** at the RHF/6-31G* level, and for benzyl radical at the ROHF/6-31G* level. Vibrational frequencies for benzene and phenyl radical have been reported previously.[20] All structures were verified to be energy minima for the given symmetries by the absence of any negative eigenvalues in the hessian matrix. Zero-point energies (ZPEs) were derived from the computed frequencies after the frequencies were scaled by a factor of 0.89.[21]

Total energies for biradicals **1**–**3**, benzene, phenyl radical, and benzyl radical were computed at the appropriate MCSCF(n,n) (n = 8, 7, or 6) level using the 6-31G* basis set as well as a correlation-consistent, polarized valence double-ζ [9s4p1d/3s2p1d] basis set for carbon[22] plus a double-ζ [4s/2s] basis set for hydrogen.[23] This latter basis set is designated pVDZ although it lacks polarization functions on hydrogen. The energies of **3**, benzene, phenyl radical, and benzyl radical, were also determined at the MCSCF(n,n) levels using a polarized valence triple-ζ [10s5p2d1f/4s3p2d1f] basis set for carbon[22] and the modified double-ζ [4s/2s] basis set for hydrogen.[23] This basis set is designated pVTZ although the f-functions on carbon were omitted. Total energies were also determined by the CISD method using the optimized (natural) molecular orbitals resolved from the appropriate MCSCF(n,n)/pVDZ calculations. Using a single reference configuration for each of the biradical triplet states and open-shell singlet states, all symmetry-allowed single and double excitations from the reference configuration were included except for those from the nonvalence molecular orbitals (frozen core approximation). Davidson-type corrections (DV2) were applied to all CISD energies in order to account for effects of quadrupule excitations.[24] In addition, the total energies of all species were evaluated using a correlation-consistent CI (CCCI) procedure similar to that described by Carter and Goddard.[25] Using the resolved natural orbitals generated from MCSCF(2,2)/6-31G* calculations, a limited CI calculation was first performed which included all symmetry-allowed configurations involving the π- and π^*-orbitals (π_1–π_7) and, for **1**–**3** and phenyl radical, the nonbonding σ-orbitals. The procedure used in this work differs somewhat from the restricted CI (RCI) approach described by Carter and Goddard in ref 25 in that each of the electrons in the active space is allowed to populate any molecular orbital in the active space rather than being restricted to pairwise excitations among the two GVB-paired molecular orbitals assigned to those particular electrons. The only difference between this limited CI and the MCSCF(n,n) procedures is that the orbitals remain unchanged in the former, whereas they are self-consistently reoptimized during the latter. In addition to the limited CI, correlation of the nonbonding σ- and π-electrons is included by allowing all single and double excitations of these electrons from the MCSCF(2,2) reference configuration (singles only for phenyl and benzyl radicals) to all of the virtual orbitals. CCCI energies were computed with a polarized, valence triple-ζ basis set, designated pVTZ′, which employed a [10s6p1d/5s3p1d] contraction on carbon and a [5s1p/3s1p] contraction on hydrogen.[23]

The Gaussian 90,[26] Gaussian 92,[27] and MOLPRO[28] programs were used for all of the geometry optimizations. The larger active space MCSCF single-point energies were computed with either the GAMESS[29] or MOLPRO codes, whereas all CISD derived energies were obtained using the MOLPRO program. All CCCI calculations employed the MELDF[30] suite of programs.

Results

The key step in the present procedure for determining heats of formation for biradicals is the measurement of an accurate threshold energy, E_T, for the collision-induced dissociation of an appropriate halocarbanion precursor. For the α,n-dehydrotoluenes, this involves the determination of halide ion dissociation energies for each of the isomeric halobenzyl anions (Scheme 1). Provided that the dissociation reactions occur efficiently to yield the desired products at the thermochemical threshold (*vide infra*), the measured values of E_T can be combined with additional data in a simple thermochemical cycle (eq 2) to derive heats of formation for each of the neutral dehydrotoluene products. Most

(17) Analysis carried out using the CRUNCH program written by Prof. P. B. Armentrout and co-workers.

(18) Chantry, P. J. *J. Chem. Phys.* **1971**, *55*, 2746.

(19) (a) Binkley, J. S.; Pople, J. A.; Hehre, W. J. *J. Am. Chem. Soc.* **1980**, *102*, 939. (b) Hehre, W. J.; Ditchfield, R.; Pople, J. A. *J. Chem. Phys.* **1972**, *56*, 2257. (c) Krishnan, R.; Frisch, M. J.; Pople, J. A. *J. Chem. Phys.* **1980**, *72*, 4244.

(20) Wierschke, S. G.; Nash, J. J.; Squires, R. R. *J. Am. Chem. Soc.* **1993**, *115*, 11958.

(21) Hout, R. F., Jr.; Levi, B. A.; Hehre, W. J. *J. Comput. Chem.* **1982**, *3*, 234.

(22) Dunning, T. H. *J. Chem. Phys.* **1989**, *90*, 1007.

(23) (a) Dunning, T. H. *J. Chem. Phys.* **1970**, *53*, 2823. (b) Dunning, T. H. *J. Chem. Phys.* **1971**, *55*, 716.

(24) (a) Langhoff, S. R.; Davidson, E. R. *Int. J. Quantum Chem.* **1974**, *8*, 61. (b) Blomberg, M. R. A.; Siegbahn, P. E. M. *J. Chem. Phys.* **1983**, *78*, 5682.

(25) (a) Carter, E. A.; Goddard, W. A. *J. Phys. Chem.* **1987**, *91*, 4651. (b) Carter, E. A.; Goddard, W. A. *J. Chem. Phys.* **1987**, *88*, 1752. (c) Carter, E. A.; Goddard, W. A. *J. Chem. Phys.* **1987**, *86*, 862. (d) Carter, E. A.; Wu, C. J. *J. Phys. Chem.* **1991**, *95*, 8352.

(26) Frisch, M. J.; Head-Gordon, M.; Trucks, G. W.; Foresman, J. B.; Schlegel, H. B.; Raghavachari, K.; Robb, M. A.; Binkley, J. S.; Gonzales, C.; Defrees, D. J.; Fox, D. J.; Whiteside, R. A.; Seeger, R.; Melius, C. F.; Baker, J.; Martin, R. L.; Kahn, L. R.; Stewart, J. J. P; Topiol, S.; Pople, J. A., GAUSSIAN 90; Gaussian, Inc.: Pittsburgh, PA, 1990.

(27) Frisch, M. J.; Head-Gordon, M.; Trucks, G. W.; Gill, P. M.; Wong, M. W.; Foresman, J. B.; Johnson, B. G.; Schlegel, H. B.; Replogle, E. S.; Gomberts, R.; Andres, J. L.; Raghavachari, K.; Robb, M. A.; Binkley, J. S.; Gonzales, C.; Defrees, D. J.; Fox, D. J.; Baker, J.; Martin, R. L.; Pople, J. A., GAUSSIAN 92, Revision A; Gaussian, Inc. Pittsburgh, PA, 1992.

(28) Developed at the University of Sussex (Falmer, Brighton, BN1 9QJ, UK) by Werner, H.-J.; Knowles, P. J., **1992**. See also: (a) Werner, H.-J.; Knowles, P. J. *J. Chem. Phys.* **1985**, *82*, 5053. (b) Werner, H.-J.; Knowles, P. J. *Chem. Phys. Lett.* **1985**, *115*, 259. (c) It should be noted that the MOLPRO program utilizes an "internally-contracted" CI algorithm, cf.: Werner, H.-J.; Knowles, P. J. *J. Chem. Phys.* **1988**, *89*, 5803; Knowles, P. J.; Werner, H.-J. *Chem. Phys. Lett.* **1985**, *145*, 514.

(29) Schmidt, M. W.; Baldridge, K. K.; Boatz, J. A.; Jensen, J. H.; Koseki, S.; Gordon, M. S.; Nguyen, K. A.; Windus, T. L.; Elbert, S. T. *QCPE Bull.* **1990**, *10*, 52.

(30) Developed at the University of Washington by McMurchie, L.; Elbert, S.; Langhoff, S.; Davidson, E. R.; Feller, D.; Rawlings, D.

$$\Delta H^\circ_{f,298}(C_6H_4CH_2) = E_T + K + \Delta H_{acid}(XC_6H_4CH_3) + \Delta H^\circ_{f,298}(XC_6H_4CH_3) - \Delta H_{acid}(HX) - \Delta H^\circ_{f,298}(HX) \quad (2)$$

of the auxiliary data in eq 2 are available in the literature[31] or can be reliably estimated[32] (Table 1). The gas-phase acidities of the halotoluenes, $\Delta H_{acid}(XC_6H_4CH_3)$, are either known or can be easily measured *via* equilibrium or bracketing techniques. The term K is required to convert E_T (= ΔE_o) to a 298 K bond dissociation enthalpy and is given by the difference in the 0–298 K integrated heat capacities for the products and reactants plus the PV work term (= RT).

One advantage of the CID threshold method of determining biradical heats of formation is its flexibility with respect to the halide leaving group used for the dissociation reaction. Thus, in principle, up to four independent measurements of each biradical heat of formation can be carried out. In the following sections, we describe our investigations of the X = Cl, Br, and I systems. We first describe gas-phase acidity measurements for nine different halotoluenes. The threshold energy measurements and data analyses are reported next, followed by a derivation of the heats of formation for the dehydrotoluenes. The calculated structures, energies, and singlet–triplet splittings of the dehydrotoluene biradicals are also described, along with the predicted heats of formation derived from isodesmic reaction analysis.

Halotoluene Acidities. Caldwell and Bartmess determined gas-phase acidities for *m*- and *p*-chlorotoluene using proton-transfer equilibrium techniques in an ICR.[33] Values for ΔG_{acid} of 366.9 ± 2.0 and 366.8 ± 2.0 kcal/mol were reported for the *meta* and *para* isomers, respectively, and the *ortho* isomer was not examined. We have determined the acidity of *o*-chlorotoluene and of each of the isomeric bromotoluenes and iodotoluenes by the bracketing technique.[31] These experiments are summarized in Table 2. The results indicate ΔG_{acid} values for all seven compounds falling between 364 and 367 kcal/mol. With neopentyl alcohol, dichloromethane, and 2-methoxyethanol, which have acidities of 366.0 ± 2.0, 366.2 ± 2.0, and 366.8 ± 2.0 kcal/mol, respectively, reversible proton transfer is observed for *o*-chlorotoluene and two of the bromotoluenes. On this basis, ΔG_{acid} values for *o*-chlorotoluene and all three bromotoluenes are assigned to be 366.5 ± 2.0 kcal/mol. The results for the iodotoluenes suggest identical acidities for the three isomers that are slightly greater than that of the chlorides and bromides; a final value for ΔG_{acid} of 365 ± 2 kcal/mol is assigned.

The ΔH_{acid} terms required for eq 2 can be obtained from the bracketed acidities using $\Delta H_{acid} = \Delta G_{acid} + T\Delta S_{acid}$. ΔS_{acid} can be reasonably estimated[34] using the relation $\Delta S_{acid} = S(H^+) + \Delta S_{rot}$, where $S(H^+)$ is the standard entropy of a proton (26.0 eu[35]) and ΔS_{rot} is the change in external and internal rotational entropy accompanying acid dissociation. A value of −1.5 eu is used to account for the loss of the methyl rotor upon ionization in all of the halotoluenes.[31] The rotational symmetry number for the *p*-halotoluenes increases from 1 to 2 upon acid dissociation, contributing $R\ln(0.5) = -0.7$ eu to ΔS_{rot}. Thus, for all of the *p*-halotoluenes, ΔS_{acid} is 23.8 eu, resulting in $T\Delta S_{acid}$ values at 298 K of 7.1 kcal/mol. This value is in good agreement with that obtained for ionization of *p*-nitrotoluene by indirect measurement in a high-pressure mass spectrometer.[36] Deprotonation of the *o*- and *m*-halotoluene isomers does not lead to a change in rotational symmetry number, so ΔS_{acid} is given by 26.0–1,5 = 24.5 eu, resulting in a $T\Delta S_{acid}$ factor at 298 K of 7.3 kcal/mol. The acidities obtained in this manner are 374 ± 2 kcal/mol for *o*-chlorotoluene, as well as for *o*-, *m*- and *p*-bromotoluene. These values are essentially the same as the ΔH_{acid} values for *m*- and *p*-chlorotoluene (374.1 ± 2.0 and 374.0 ± 2.0 kcal/mol, respectively) reported by Caldwell and Bartmess.[33] For *o*-, *m*- and *p*-iodotoluene, the final acidities are 372 ± 2 kcal/mol.

Table 1. Supplemental Thermochemical Data

compd	$\Delta H^\circ_{f,298}$(g), kcal/mol	ref
$ClC_6H_4CH_3$	4.7 ± 1.0	*a*
$BrC_6H_4CH_3$	17 ± 1	*a*
$IC_6H_4CH_3$	31 ± 1	*a*
HCl	−22.1 ± 0.04	*b*
HBr	−8.7 ± 0.1	*b*
HI	6.3 ± 0.1	*b*
C_6H_6	19.7 ± 0.2	*c*
$C_6H_5CH_3$	12.0 ± 0.1	*c*
C_6H_5	78.9 ± 0.8	*d*
$C_6H_5CH_2$	48.4 ± 1.5	*e*
H	52.1	*b*
compd	**ΔH_{acid}, kcal/mol**	**ref**
HCl	333.4 ± 0.2	*f*
HBr	323.6 ± 0.3	*f*
HI	314.4 ± 0.1	*f*

[a] Heats of formation of *ortho*, *meta*, and para isomers are the same within 0.5 kcal/mol, refs 31, 32. [b] Reference 35. [c] Pedley, J. B.; Naylor, R. D.; Kirby, S. P. *Thermochemistry of Organic Compounds*, 2nd ed.; Chapman and Hall: New York, NY, 1986. [d] Reference 41. [e] Reference 44. [f] Reference 31.

Energy-Resolved Collision-Induced Dissociation. Collision-induced dissociation of a halobenzyl anion (X = Cl, Br, I) yields the corresponding halide ion as the only observed ionic fragment over the 0.5–6 eV (center-of-mass frame) energy range. The energy-resolved CID cross sections for the *o*-, *m*- and *p*-halobenzyl anions are shown in Figures 1a–1c, where 1a, 1b, and 1c are for chloro-, bromo-, and iodobenzyl anions, respectively. The maximum CID cross sections range from *ca.* 3 to 6 Å^2, with the chlorobenzyl anions exhibiting the lowest cross sections and the iodobenzyl anions showing the highest. *o*-, *m*-, and *p*-fluorobenzyl anions were also briefly examined. These ions exhibit anomalous behavior in that the F^- appearance curves are characterized by significantly lower cross sections ($\sigma_{max} \approx 0.1$ Å^2) and slowly rising onsets with apparent dissociation thresholds greater than 5 eV—more than 2 eV above the expected values based on the results for the other halides (*vide infra*). This is reminiscient of the behavior of fluorophenyl anions encountered in our earlier study of benzyne thermochemistry[2b] and is attributed to a competitive shift[37] due to collision-induced electron detachment from the activated fluorobenzyl anions. Because no useful thermochemical information can be derived from the fluorobenzyl anion CID data, these ions were not examined further.

The Cl^-, Br^-, and I^- appearance curves were modeled using eq 1. As described in the Experimental Section, this model function includes the reactant ion internal energy contribution and the dissociation probabilities determined by RRKM calculations. Using the scaled molecular vibrational frequencies obtained from MOPAC/AM1 calculations, the average internal energies of the halobenzyl anions are found to be in the range 0.12–0.13 eV (2.8–3.1 kcal/mol). For RRKM lifetime analyses, some assumptions regarding the nature of the dissociation transition-state are required, and the results for some systems can be quite sensitive to the exact choice of transition-state parameters. The relative "tightness" or "looseness" of the dissociation transition

(31) Lias, S. G.; Bartmess, J. E.; Liebman, J. F.; Holmes, J. L.; Levin, R. D.; Mallard, W. G. *J. Phys. Chem. Ref. Data* **1988**, *17*, Suppl. 1. All data taken from the NIST Negative Ion Energetics Database, Version 3.00, NIST Standard Reference Database 19B, October, 1993.

(32) (a) Benson, S. W. *Thermochemical Kinetics*; John Wiley & Sons: New York, 1976. (b) Benson, S. W.; Garland, L. J. *J. Phys. Chem.* **1991**, *95*, 4915.

(33) Caldwell, G.; Bartmess, J. E., unpublished results tabulated in ref 31.

(34) Bartmess, J. E.; McIver, R. T., Jr. In *Gas Phase Ion Chemistry*, Vol. 2; Bowers, M. T., Ed.; Academic Press: New York, NY, 1979; Chapter 11.

(35) Chase, M. W.; Davies, C. A.; Downey, J. R.; Frurip, D. J.; McDonald, R. A.; Syverud, A. N. *J. Phys. Chem. Ref. Data*, **1985**, *14*, Suppl. 1 (JANAF Tables).

(36) Cumming, J. B.; Kebarle, P. *Can. J. Chem.* **1978**, *56*, 1.

(37) Lifshitz, C.; Long, F. A. *J. Chem. Phys.* **1964**, *41*, 2468.

Table 2. Summary of Acid–Base Bracketing Experiments for *o*-, *m*-, and *p*-Halotoluenes[a]

$$XC_6H_4CH_2^- + HA \rightleftharpoons XC_6H_4CH_3 + A^-$$

HA	$\Delta G_{acid}(HA)$[b]	*o*-chloro		*o*-bromo		*m*-bromo		*p*-bromo	
		forward	reverse	forward	reverse	forward	reverse	forward	reverse
MeOH	374.0 ± 2.0	–	+	–	+	–	+	–	+
EtOH	370.8 ± 2.0	–	+	–	+	–	+	–	+
n-PrOH	369.4 ± 2.0	–	+	–	+	–	+	–	+
i-PrOH	368.8 ± 2.0	–	+	–	+	–	+	–	+
t-BuOH	368.0 ± 2.0	–	+	–	+	–	+	–	+
n-pentyl alcohol	367.3 ± 2.0	–	+	–	+	–	+	–	+
$MeOCH_2CH_2OH$	366.8 ± 2.0	–	–	+ (slow)[c]	+	+	+	+	+
CH_2Cl_2	366.2 ± 2.0[d]	+	–	+	–	+	+	+	+
neopentyl alcohol	366.0 ± 2.0	+	+ (slow)[c]	+	–	+	+ (slow)[c]	+	+
acetonitrile	365.2 ± 2.0	+	–	+	–	+	–	+	–
acetone	361.9 ± 2.0	+	–	+	–	+	–	+	–

HA	$\Delta G_{acid}(HA)$[b]	*o*-iodo		*m*-iodo		*p*-iodo	
		forward	reverse	forward	reverse	forward	reverse
MeOH	374.0 ± 2.0	–	+	–	+	–	+
EtOH	370.8 ± 2.0	–	+	–	+	–	+
i-PrOH	368.8 ± 2.0	–	+	–	+	–	+
$MeOCH_2CH_2OH$	366.8 ± 2.0	–	+	–	+	–	+
CH_2Cl_2	366.2 ± 2.0[d]	–	+	–	+	–	+
acetonitrile	365.2 ± 2.0	–	+	–	+	+	+
FCH_2CH_2OH	364.6 ± 2.0	+	–	+	–	+	–
3,3-dimethyl-2-butanol	364.5 ± 2.0	+	–	+	–	+	–
acetone	361.9 ± 2.0	+	–	+	–	+	–
2-butanone	361.3 ± 2.0	+	–	+	–	+	–
acetaldehyde	359.0 ± 2.0	+	–	+	–	+	–

[a] All experiments carried out in the flowing afterglow at 298 K; + and – correspond to observance and nonobservance of proton transfer, respectively. [b] Values in kcal/mol; taken from ref 31 unless otherwise noted. [c] By "slow" it is meant that while proton transfer is observed, it does so at an apparent rate that is less than that for the reverse proton-transfer reaction under conditions of comparable neutral flow. [d] Reference 1c.

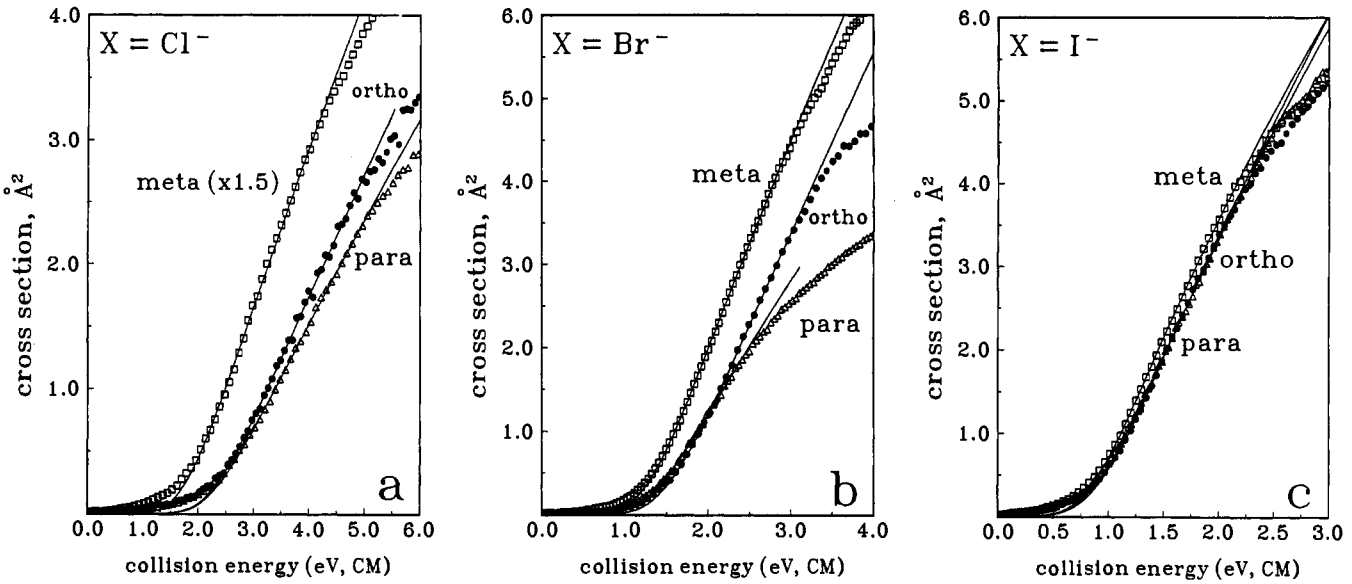

Figure 1. Cross sections for dissociation of halide ion from *o*-, *m*-, and *p*-halobenzyl anions resulting from collisional activation with argon target at (3–5) × 10^{-5} Torr. The solid lines are the optimized, fully convoluted model appearance curve obtained with the model indicated in eq 1 and described in the text: (a) chlorobenzyl anions, (b) bromobenzyl anions, (c) iodobenzyl anions.

state is reflected by the activation entropy, $\Delta S^{\ddagger}$, which can be estimated from the vibrational partition functions for the reactant ion (Q) and transition state ($Q^{\ddagger}$) as in eq 3, where $q_i = 1/[1 - \exp(-h\nu/k_BT)]$ and $E_v^{\ddagger}$ and E_v are the average vibrational energies of the transition state and reactant ion, respectively, and k_B is the Boltzmann constant. By convention, the activation entropy is

$$\Delta S^{\ddagger} = k_B \ln(Q^{\ddagger}/Q) + (E_v^{\ddagger} - E_v)/T = k_B \ln(\prod q_i^{\ddagger}/\prod q_i) + (E_v^{\ddagger} - E_v)/T \quad (3)$$

evaluated at 1000 K; values of $\Delta S^{\ddagger}_{1000}$ are negative for tight transition states and positive for loose transition states.[38] In keeping with our previous studies of collisionally-activated halide elimination reactions of halophenyl anions,[2b] we assume a "product-like" transition state for halobenzyl anion dissociation that is characterized by the vibrational frequencies of the product dehydrotoluene plus two additional low frequencies of 25 cm^{-1} to represent in-plane and out-of-plane bending of the dissociating carbon–halide bond. This particular choice of bending frequencies gives $\Delta S^{\ddagger}_{1000}$ values for the halobenzyl anion dissociations in the range 5.7–8.2 eu. This same range for $\Delta S^{\ddagger}_{1000}$ was used in our

(38) Lifshitz, C. *Adv. Mass Spectrom.* **1989**, *7*, 713.

Table 3. CID Threshold Energies for Halobenzyl Anions, Fitting Parameters, Halide Dissociation Enthalpies, and Derived Heats of Formation for α,2-, α,3-, and α,4-Dehydrotoluene

halobenzyl anion	E_T,[a] kcal/mol	n[b]	$\Delta S^{\ddagger}_{1000}$,[c] eu	$DH_{298}[CH_2C_6H_4-X^-]$,[d] kcal/mol	$\Delta H^{\circ}_{f,298}(C_6H_4CH_2)$,[e] kcal/mol
o-Cl	40.7 ± 2.1	1.66 ± 0.08	7.8	41.4 ± 2.1	109 ± 3
m-Cl	33.4 ± 2.8	1.70 ± 0.08	8.2	34.2 ± 2.8	102 ± 3
p-Cl	40.7 ± 1.2	1.70 ± 0.07	7.6	41.4 ± 1.2	109 ± 3
o-Br	30.0 ± 1.6	1.69 ± 0.12	6.7	30.6 ± 1.6	107 ± 3
m-Br	27.3 ± 2.8	1.64 ± 0.09	7.2	28.0 ± 2.8	104 ± 3
p-Br	27.4 ± 2.3	1.72 ± 0.07	6.4	28.0 ± 2.3	104 ± 3
o-I	20.1 ± 2.3	1.67 ± 0.17	6.0	20.6 ± 2.3	103 ± 3
m-I	20.5 ± 2.3	1.59 ± 0.11	6.7	21.1 ± 2.3	103 ± 3
p-I	20.6 ± 1.4	1.68 ± 0.07	5.7	21.1 ± 2.3	103 ± 3

[a] Average threshold energy (0 K) for halide elimination determined by the methods outlined in ref 2b. [b] Exponential fitting parameter from eq 1. [c] Dissociation activation entropy used for RRKM analysis calculated with eq 3. [d] Halide dissociation enthalpy (298 K) derived from E_T value. [e] Dehydrotoluene heat of formation calculated from eq 2; see text for discussion of uncertainties.

Table 4. Optimized C–C Bond Lengths (Å) for 1–3, Benzene, Phenyl Radical, and Benzyl Radical

compd	method	state	C_α–C_1	C_1–C_2	C_2–C_3	C_3–C_4	C_4–C_5	C_5–C_6	C_6–C_1
1 (C_s)	MCSCF(2,2)/6-31G*	$^3A''$	1.444	1.383	1.371	1.389	1.390	1.382	1.404
		$^1A''$	1.454	1.389	1.364	1.396	1.383	1.390	1.396
	MCSCF(8,8)/3-21G	$^3A''$	1.399	1.414	1.382	1.400	1.412	1.382	1.436
		$^1A''$	1.427	1.417	1.360	1.426	1.384	1.408	1.408
1 (C_s)	MCSCF(2,2)/6-31G*	$^1A'$	1.343	1.468	1.439	1.355	1.445	1.336	1.460
2 (C_s)	MCSCF(2,2)/6-31G*	$^3A''$	1.448	1.402	1.369	1.373	1.391	1.384	1.400
		$^1A''$	1.449	1.402	1.368	1.373	1.391	1.385	1.399
	MCSCF(8,8)/3-21G	$^3A''$	1.411	1.429	1.374	1.390	1.406	1.389	1.425
		$^1A''$	1.400	1.432	1.375	1.391	1.410	1.386	1.434
2 (C_1)	RHF/6-31G*	^1A	1.328	1.492	1.316	1.316	1.482	1.336	1.494
3 (C_{2v})	MCSCF(2,2)/6-31G*	$^3B_1$	1.446	1.400	1.386	1.373			
		$^1B_1$	1.454	1.389	1.364	1.396			
	MCSCF(8,8)/3-21G	$^3B_1$	1.399	1.433	1.385	1.396			
		$^1B_1$	1.445	1.411	1.401	1.381			
3 (C_{2v})	MCSCF(2,2)/6-31G*	$^1A_1$	1.333	1.459	1.340	1.461			
benzene (D_{6h})[a]	RHF/6-31G*	$^1A_{1g}$		1.386					
	MCSCF(6,6)/3-21G	$^1A_{1g}$		1.395					
phenyl (C_{2v})[a]	ROHF/6-31G*	$^2B_1$		1.373	1.390	1.388			
	MCSCF(7,7)/3-21G	$^2B_1$		1.384	1.400	1.398			
benzyl (C_{2v})	ROHF/6-31G*	$^2B_1$	1.449	1.398	1.383	1.387			
	MCSCF(7,7)/3-21G	$^2B_1$	1.409	1.424	1.386	1.402			

[a] Reference 20.

earlier studies of halophenyl anion CID,[2b] and it is quite similar to the range for $\Delta S^{\ddagger}_{1000}$ determined from *time-resolved* photodissociation experiments with bromo- and chlorobenzene cations, wherein dissociation lifetime effects can be quantified.[39]

The optimized values for E_T and n obtained from fits of the data to eq 1 and the corresponding $\Delta S^{\ddagger}_{1000}$ values computed from eq 3 for each of the nine halobenzyl anions are summarized in Table 3. These thresholds correspond to the dissociation energies at 0 K. They may be converted to 298 K dissociation enthalpies by correcting for the differences in integrated heat capacities between the products and reactants and by adding an expansion–work term equal to RT. The resulting values for $DH_{298}[CH_2C_6H_4-X^-]$ are also listed in Table 3. The *apparent* heats of formation for the neutral dehydrotoluene products, calculated according to eq 2 from the halobenzyl anion dissociation enthalpies, the halotoluene acidities, and the auxiliary data in Table 1, are listed in the last column of Table 3.

Computational Results. The optimized C–C bond lengths obtained for the triplet and open-shell singlet states of **1–3**, and for benzene, phenyl radical, and benzyl radical, determined with the two different levels of theory, are listed in Table 4. In addition, the C–C bond lengths and selected bond angles obtained at the MCSCF(n,n)/3-21G level are shown in Figure 2. The C–C bond lengths obtained at the MCSCF(2,2)/6-31G* or the RHF/6-31G* level for the closed-shell singlet states of **1–3** are also listed in Table 4. The numbering scheme used in the table for the dehydrotoluenes is shown below (the numbering is analogous for ^{1}A **2**). Complete lists of all geometrical parameters and vibrational frequencies are available as supplementary material.[40]

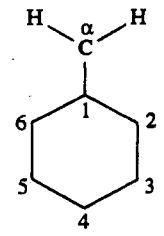

Total energies for the singlet and triplet states of **1–3** were computed at the MCSCF(8,8)/6-31G* level using the MCSCF(2,2)/6-31G* optimized geometries and at the MCSCF(8,8)/pVDZ, CISD+DV2/pVDZ and CCCI/pVTZ′ levels of theory using the MCSCF(8,8)/3-21G optimized geometries. The total energies of the singlet and triplet states of **3** were also determined at the MCSCF(8,8)/pVTZ//MCSCF(8,8)/3-21G level. These data are listed in Table 5, along with the MCSCF(2,2)/6-31G* energies for the closed-shell singlet states of **1** and **3** and the RHF/6-31G* energy for ^{1}A **2**. The singlet–triplet gaps (ΔE_{ST})

(39) (a) Malinovich, Y.; Arakawa, R.; Haase, G.; Lifshitz, C. *J. Phys. Chem.* **1985**, *89*, 2253. (b) Pratt, S. T.; Chupka, W. A. *Chem. Phys.* **1981**, 153. (c) Gotkis, Y.; Naor, M.; Laskin, J.; Lifshitz, C.; Faulk, J. D.; Dunbar, R. C. *J. Am. Chem. Soc.* **1993**, *115*, 7402.

(40) Ordering information is given on any current masthead page.

Table 5. Total Energies, Singlet–Triplet Splittings, BSE Values, and Calculated Heats of Formation for 1–3[a]

compd	theory level	state	$-E_{tot}$	ZPE[b]	ΔE_{ST}[c]	BSE[d]	$\Delta H°_{f,298}$[e]
1 (C_s)	MCSCF(2,2)/6-31G*[f]	$^3A''$	268.463 48	60.6	−2.53	0.78	106.8
		$^1A''$	268.459 45	60.6		−1.75	109.4
	MCSCF(8,8)/6-31G*[f]	$^3A''$	268.546 71		−6.86	1.98	105.6
		$^1A''$	268.535 77			−4.89	112.5
	MCSCF(8,8)/pVDZ[g]	$^3A''$	268.565 25		−7.40	2.23	105.4
		$^1A''$	268.553 45			−5.18	112.8
	CISD+DV2/pVDZ[g]	$^3A''$	269.352 93		−4.11	1.05	106.5
		$^1A''$	269.346 38			−3.06	110.7
	CCCI/pVTZ'[g]	$^3A''$	268.577 81		−4.22	1.26	106.3
		$^1A''$	268.571 09			−2.96	110.6
1 (C_s)	MCSCF(2,2)/6-31G*[f]	$^1A'$	268.434 11				
2 (C_s)	MCSCF(2,2)/6-31G*[f]	$^3A''$	268.462 62	60.6	−0.39	0.24	107.4
		$^1A''$	268.462 00	60.6		−0.15	107.8
	MCSCF(8,8)/6-31G*[f]	$^3A''$	268.542 69		2.52	−0.55	108.2
		$^1A''$	268.546 70			1.97	105.6
	MCSCF(8,8)/pVDZ[g]	$^3A''$	268.560 67		3.02	−0.65	108.3
		$^1A''$	268.565 48			2.37	105.2
	CISD+DV2/pVDZ[g]	$^3A''$	269.351 67		0.31	0.26	107.3
		$^1A''$	269.352 17			0.58	107.0
	CCCI/pVTZ'[g]	$^3A''$	268.575 42		0.95	−0.24	107.8
		$^1A''$	268.576 94			0.72	106.9
2 (C_1)	RHF/6-31G*[f]	^1A	268.408 98				
3 (C_{2v})	MCSCF(2,2)/6-31G*[f]	$^3B_1$	268.462 49	60.7	−1.54	0.06	107.5
		$^1B_1$	268.459 72	60.5		−1.48	109.1
	MCSCF(8,8)/6-31G*[f]	$^3B_1$	268.546 09		−6.76	1.49	106.1
		$^1B_1$	268.534 99			−5.28	112.9
	MCSCF(8,8)/pVDZ[g]	$^3B_1$	268.565 06		−8.05	2.01	105.6
		$^1B_1$	268.551 93			−6.04	113.6
	MCSCF(8,8)/pVTZ[g]	$^3B_1$	268.605 58		−8.18	2.07	105.5
		$^1B_1$	268.592 23			−6.11	113.7
	CISD+DV2/pVDZ[g]	$^3B_1$	269.352 39		−3.10	0.62	107.0
		$^1B_1$	269.347 17			−2.49	110.1
	CCCI/pVTZ'[g]	$^3B_1$	268.578 16		−4.99	1.38	106.2
		$^1B_1$	268.569 89			−3.61	111.2
3 (C_{2v})	MCSCF(2,2)/6-31G*[f]	$^1A_1$	268.434 14				

[a] Total energies in atomic units; all other quantities in kcal/mol. [b] Computed from MCSCF(2,2)/6-31G* frequencies. [c] $(E_{tot} + ZPE)_{triplet} - (E_{tot} + ZPE)_{singlet}$. [d] Biradical separation energy defined in Scheme 2, corrected to 298 K. [e] Calculated from 298 K BSE value and auxiliary data according to eq 4. [f] Calculated single-point energies using MCSCF(2,2)/6-31G* optimized geometries. [g] Calculated single-point energies using MCSCF(8,8)/3-21G optimized geometries.

for **1–3** are calculated from $\Delta E_{ST} = (E_{tot} + ZPE)_{triplet} - (E_{tot} + ZPE)_{singlet}$ and are also given in Table 5 for each computational level. Note that a positive value for ΔE_{ST} means that the singlet state is lower in energy than the triplet state. The RHF, ROHF, MCSCF, CISD, and CCCI energies for benzene,[20] phenyl radical,[20] and benzyl radical, computed with these same basis sets and analogous MCSCF active spaces, are given in Table 6.

Following the prescription developed earlier for the benzynes,[20] the absolute heats of formation for the dehydrotoluene biradicals were calculated from the computed energy change for the isodesmic reaction shown in Scheme 2, termed the *biradical separation energy (BSE)*. This quantity provides a direct measure of the stabilization or destabilization involved when the two radical centers are in the same molecule compared to two separate radicals. A positive value for the BSE indicates that the biradical is stabilized relative to simple bond energy additivity ("noninteracting biradical") models, and a negative value indicates that it is destabilized. The calculated BSE values, which include the appropriate ΔZPE and 298 K temperature corrections, are listed in Table 5 for the singlet and triplet states of the three dehydrotoluenes. They may be combined with the standard heats of formation of benzene, phenyl radical, and benzyl radical listed in Table 1 according to eq 4 to derive the standard heats of formation of **1–3**. The value used here for the heat of formation

$$\Delta H°_{f,298}(\mathbf{1, 2, \text{or } 3}) = \Delta H°_{f,298}(C_6H_5) + \Delta H°_{f,298}(C_6H_5CH_2) - \Delta H°_{f,298}(C_6H_6) - \text{BSE}(\mathbf{1, 2, \text{or } 3}) \quad (4)$$

of phenyl radical is based upon $DH_{298}[C_6H_5\text{–H}] = 111.2 \pm 0.8$ kcal/mol,[41–46] and the value for benzyl radical is derived from $DH_{298}[C_6H_5CH_2\text{–H}] = 88.5 \pm 1.5$ kcal/mol.[44] The heats of formation for the dehydrotoluenes calculated with eq 4 can thus be directly compared to the values obtained from experiment. The derived heats of formation for the singlet and triplet states of **1–3** are listed in the last column of Table 5.

Table 6. Total Energies and Zero-Point Energies for Benzene, Phenyl Radical, and Benzyl Radical

compd	theory level	$-E_{tot}$, au	ZPE,[a] kcal/mol
benzene (D_{6h})[b]	RHF/6-31G*[c]	230.703 14	60.1
	MCSCF(6,6)/6-31G*[c]	230.775 85	
	MCSCF(6,6)/pVDZ[d]	230.789 11	
	MCSCF(6,6)/pVTZ[d]	230.824 19	
	CISD+DV2/pVDZ[d]	231.497 17	
	CCCI/pVTZ'[d]	230.826 40	
phenyl (C_{2v})[b]	ROHF/6-31G*[c]	230.050 91	52.5
	MCSCF(7,7)/6-31G*[c]	230.126 29	
	MCSCF(7,7)/pVDZ[d]	230.140 40	
	MCSCF(7,7)/pVTZ[d]	230.175 48	
	CISD+DV2/pVDZ[d]	230.823 74	
	CCCI/pVTZ'[d]	230.174 03	
benzyl (C_{2v})	ROHF/6-31G*[c]	269.114 47	68.2
	MCSCF(7,7)/6-31G*[c]	269.193 12	
	MCSCF(7,7)/pVDZ[d]	269.210 41	
	MCSCF(7,7)/pVTZ[d]	269.250 83	
	CISD+DV2/pVDZ[d]	270.024 68	
	CCCI/pVTZ'[d]	269.228 17	

[a] Computed from RHF/6-31G* or ROHF/6-31G* frequencies. [b] Reference 20. [c] Calculated single-point energies using MCSCF(2,2)/6-31G* optimized geometries. [d] Calculated single-point energies using MCSCF(8,8)/3-21G optimized geometries.

Scheme 2

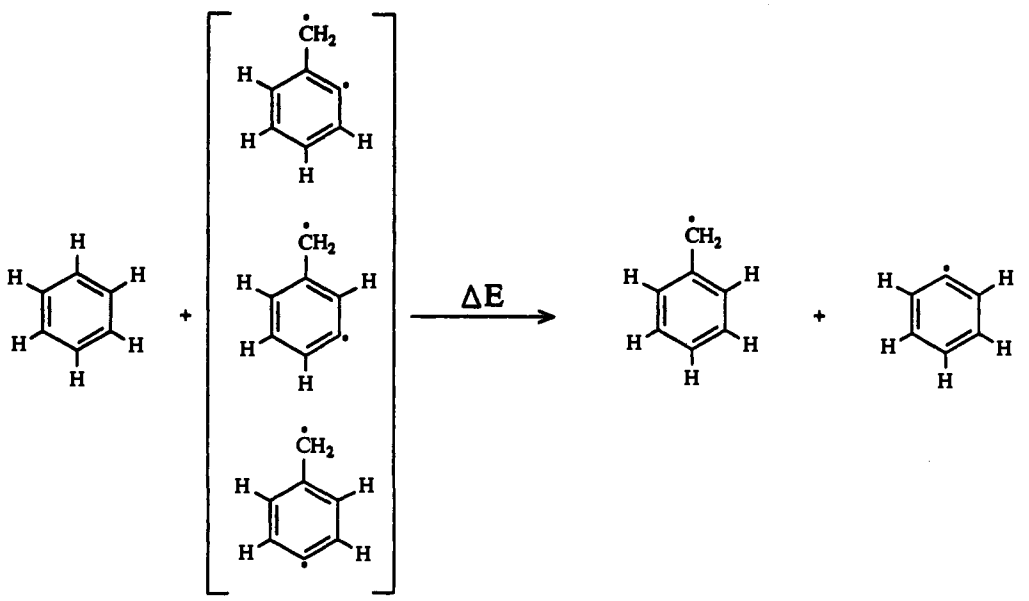

Discussion

The most striking feature in the experimental data is the pronounced change in the *relative* halide ion dissociation energies for the three halobenzyl anions (Figure 1). A decrease in the absolute dissociation energies in going from Cl^- to Br^- to I^- is to be expected since covalent and electrostatic binding of a halide ion to carbon always decreases with increasing atomic number. However, the appearance curves in Figure 1 show that the *o*- and *p*-chlorobenzyl anions have nearly identical Cl^- dissociation energies that are *ca.* 0.3 eV greater than that for the *meta* isomer, while the three isomeric iodobenzyl anions have essentially the same I^- dissociation energy. Because the gas-phase acidities of all the halotoluenes are similar, the apparent heats of formation derived for **1** and **3**, but not **2**, display a dependence on the halide ion leaving group (Table 3). We interpret this to mean that the *o*- and *p*-halobenzyl anion dissociation reactions are subject to some mechanistic or dynamical constraints not present with *m*-halobenzyl anions that cause either reverse activation energies and/or kinetic shifts in their dissociation onsets. In this regard, the results of the electronic structure calculations for **1–3** provide several useful insights. However, before addressing this point further, we first present a brief discussion of some of the general characteristics of halobenzyl anion dissociation relating to electron detachment and possible alternative product structures. We then provide a summary of the computational results and select the best theoretical method from those employed for comparison with experiment.

Electron Detachment. A potential complication in CID threshold measurements with negative ions is collision-induced electron detachment from the reactant ion, since this could suppress the total reaction cross section and lead to a competitive shift in the dissociation onset.[37] In previous investigations of metal carbonyl anions[10,11] and other types of halocarbanions,[1] we concluded that collision-induced electron detachment becomes a complication only when the activation energy for the dissociation reaction of interest exceeds the electron detachment energy by a large margin (*ca.* 1 eV). The electron binding energies of halobenzyl anions are not known independently, but they can be reasonably estimated to be in the range of 1.0–1.2 eV (23–28 kcal/mol) from the measured halotoluene acidities and an estimate for the benzylic C–H bond strength of about 88 kcal/mol. Thus, only in the case of the *o*- and *p*-chlorobenzyl anions does the apparent CID threshold energy significantly exceed the electron binding energy, but by no more than about 0.7 eV. However, the fact that the total CID cross sections measured for all the halobenzyl anions are not especially low, and that the *m*-chlorobenzyl anion isomer shows a much lower threshold energy despite its having roughly the same electron binding energy as the *ortho* and *para* ions lead us to conclude that electron detachment is unimportant in the chloro-, bromo- and iodobenzyl anion systems. For the fluorobenzyl anions, the estimated F^- dissociation energies based on $\Delta H_{acid}(FC_6H_4CH_3) \approx 377$ kcal/mol and $\Delta H_f(C_6H_4CH_2) = 103$ kcal/mol (Table 3) are about 3 eV. This is about 2 eV higher than the estimated electron binding energy for a halobenzyl anion. Therefore, collision-induced electron loss is likely to be rapid at the true F^- dissociation threshold, an effect which probably accounts for the extremely low CID cross sections observed with these ions and the pronounced (>2 eV) shifts in the F^- dissociation onsets.

Product Structures. Because the neutral product formed from CID of the halobenzyl anions is not detected directly, we must validate our assumption that dehydrotoluene biradicals are formed rather than some other C_7H_6 isomer(s). However, at the outset it should be noted that all alternative product structures require skeletal and/or hydrogen rearrangements during dissociation. Such processes will generally involve much tighter transition states than the simple bond cleavages that produce dehydrotoluene biradicals and therefore would be expected to be much less efficient unless their activation energies are unusually low. The observed CID cross sections of 3–6 $Å^2$ are probably too high for dissociative rearrangements.[47] Nevertheless, many of the conceivable alternative C_7H_6 isomers can be directly ruled out on simple energetic grounds. For example, (*Z*)-1,2,4-heptatrien-6-yne, a

(41) The magnitude of the C–H bond strength in benzene has been somewhat controversial.[42-44] The value used in this work ($DH_{298}[C_6H_5–H] = 111.2 \pm 0.8$ kcal/mol) is derived from the gas-phase acidity of benzene ($\Delta H_{acid}(C_6H_6)$), the electron affinity of phenyl radical ($EA(C_6H_5)$), and the ionization potential of hydrogen (IP(H)) according to the relation,[34] $DH[C_6H_5–H] = \Delta H_{acid}(C_6H_6) + EA(C_6H_5) - IP(H) + T_{corr}$, and using the data $\Delta H_{acid}(C_6H_6) = 399.8 \pm 0.7$ kcal/mol,[45] $EA(C_6H_5) = 25.3 \pm 0.1$ kcal/mol,[46] IP(H) = 313.6 kcal/mol, and $T_{corr} = \int C_p(C_6H_5) - \int C_p(C_6H_5–) = -0.25$ kcal/mol.[44]

(42) McMillen, D. F.; Golden, D. M. *Annu. Rev. Phys. Chem.* **1982**, *33*, 493.

(43) Robaugh, D.; Tsang, W. *J. Phys. Chem.* **1986**, *90*, 5363.

(44) Berkowitz, J.; Ellison, G. B.; Gutman, D. *J. Phys. Chem.* **1994**, *98*, 2744. We thank Professor Ellison for a preprint of this comprehensive review.

(45) Meot-Ner, M; Kafafi, S. A. *J. Am. Chem. Soc.* **1988**, *110*, 6297. The acidity reported in this paper refers to 600 K and has been corrected to 298 K by G. B. Ellison, cf. ref 44.

(46) Gunion, R. F.; Gilles, M. K.; Polak, M. L.; Lineberger, W. C. *Int. J. Mass Spectrom. Ion Process* **1992**, *117*, 601.

ring-opening product that could form by a Grob-like fragmentation of a *m*-halobenzyl anion, has an estimated heat of formation of 118 kcal/mol[32]—a value that is much higher than any of the measured heats of formation. All other acyclic C_7H_6 isomers are too high in energy as well. It seems safe to rule out any isomers requiring hydrogen rearrangements since, unlike in cations, proton shifts in anions and hydrogen atom shifts in neutral radicals have very high barriers (40–60 kcal/mol)[48] —too high to be accommodated by the measured CID threshold energies. Note that base catalysis of such processes by the nascent halide ions formed during decomposition is unlikely due to the extremely low proton affinities of these ions.[31] Thus, phenyl carbene (ΔH_f = 106 ± 3 kcal/mol[49]), ethynylcyclopentadienes ($\Delta H_f \approx$ 90 kcal/mol[32]), and 1,2,4,6-cycloheptatetraene (ΔH_f = 92 kcal/mol[50]), to name a few, can be ruled out on this basis.

Two low-energy C_7H_6 isomers exist that are at least conceivable mechanistically: benzocyclopropene (**4**, ΔH_f = 89 ± 1 kcal/mol[51]) and fulvenallene (5-vinylidene-1,3-cyclopentadiene, **5**, ΔH_f = 82 ± 2 kcal/mol[31]). The former could arise from an

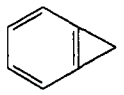

4

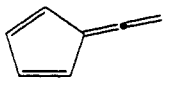

5

o-halobenzyl anion by twisting of the benzylic anion followed by an intramolecular nucleophilic displacement of the *o*-halide, while the latter might form from an *o*-halobenzyl anion by a Favorskii-like, anionic 1,2-vinyl shift of the C-6 carbon to C-2 with accompanying ejection of the halide ion. The measured CID thresholds for the *o*-halobenzyl anions and the C_7H_6 heats of formation derived from them (Table 3) would therefore require that these rearrangement reactions have activation energies of 14–25 kcal/mol or, alternatively, that they have even lower barriers but are slow enough to induce corresponding kinetic shifts in the dissociation onsets. For a number of reasons, such low barriers for these reactions are unlikely. Thermal ring contraction of *ortho*-substituted benzylic anions to form fulvenallenes is unprecedented in solution. The reaction involves not only loss of benzylic resonance in the reactant (*ca.* 28 kcal/mol[52]), since the CH_2 group is orthogonal to the ring plane in the product, but also complete disruption of the aromatic ring. A search for the transition state for this reaction with MOPAC/AM1 semiempirical calculations suggests an activation energy of no less than 100 kcal/mol—far greater than any of the measured X^- appearance energies. Formation of benzocyclopropene from *o*-halobenzyl anions is also unprecedented in solution, although ring closure of *o*-(methoxymethyl)phenyllithium reagents has been observed.[53] Cyclopropene ring formation in this system also requires substantial twisting of the benzylic CH_2 group and loss of π-conjugation, as well as a disfavorable intramolecular displacement involving a *syn* nucleofuge. Furthermore, MOPAC/AM1 calculations indicate that this rearrangement reaction has an activation energy of about 70 kcal/mol—a value that is also much higher than any of the measured CID thresholds. Thus, reasonable mechanistic considerations and theoretical estimates of the required activation energies suggest that both **4** and **5** can be ruled out as neutral products from CID of *o*-halobenzyl ions. In the absence of any evidence to the contrary, we shall assume that the measured CID threshold energies correspond to the kinetically-preferred, direct cleavage of the carbon–halide bonds to form dehydrotoluene biradicals.

Dehydrotoluene Biradicals: Geometries and Electronic Structures. A partial listing of the results of the geometry optimizations for **1–3**, benzene, phenyl radical, and benzyl radical using the two different computational procedures is given in Table 4. In general, the C–C bond distances for the triplet and open-shell singlet states of **1–3** obtained from the MCSCF(2,2)/6-31G* calculations are less varied than those obtained from the MCSCF-(8,8)/3-21G optimizations, and they more closely resemble the ROHF/6-31G* optimized structure for benzyl radical. For example, the exocyclic C_α–C_1 bond distances obtained at the MCSCF(2,2)/6-31G* level for both the singlet and the triplet states of **1–3** are all nearly the same (1.449 ± 0.005 Å) and are essentially identical to the ROHF bond distance computed for benzyl radical (1.449 Å). Moreover, the extent of C–C bond length alternation is clearly lower in the MCSCF(2,2)/6-31G* structures than in the MCSCF(8,8)/3-21G structures. The MCSCF(2,2)/6-31G* structures for **2** are very similar to the optimized structure for singlet **2** obtained by Koga and Morokuma from MCSCF(4,4)/MIDI1 calculations.[54] The differences between the MCSCF(2,2) and MCSCF(8,8) geometries are a natural consequence of the fact that the larger active space calculations include configurations involving excitations into the π^*-orbitals, whereas the MCSCF(2,2) calculations do not. The partial occupation of the antibonding π^*-orbitals and accompanying depopulation of the π- and σ-orbitals lessens the energetic costs of C–C skeletal deformations. In our recent computational study of the benzynes,[20] we selected the geometries obtained from MCSCF(8,8)/3-21G optimizations as the most physically realistic, in part because of the excellent agreement between the MCSCF(6,6)/3-21G derived C–C bond length for benzene (1.395 Å) and the experimental value (1.397 Å).[55] Furthermore, Jordan and co-workers previously noted the importance of including the π- and π^*-orbitals in the active space used for MCSCF geometry optimizations involving tetramethyleneethane and cyclopentadienyltrimethylenemethane biradicals.[56] Accordingly, we have chosen the MCSCF(8,8)/3-21G derived geometries for **1–3** as the most accurate and have used these structures for all subsequent energy calculations.

The structures obtained for **1–3** from the MCSCF(8,8)/3-21G calculations shown in Figure 2 display several notable features. The geometries computed for the triplet and open-shell singlet states of **1** and **3** are clearly different, whereas the optimized structures for the open-shell singlet and triplet states of **2** are essentially the same. For example, the C_α–C_1 bond lengths in the triplet states of **1** and **3** are shorter than those in the singlet states by 0.03–0.05 Å. In general, the structures for triplets **1** and **3** resemble triplet methylenecyclohexadienylidenes, while the open-shell singlet-state structures indicate a lesser extent of π-delocalization between the exocyclic carbon and the aromatic ring. On the other hand, the computed structures for the open-shell singlet state and the triplet state of **2** are most similar to that of benzyl radical, except for the slightly shorter C–C bonds about the dehydrocarbon atoms that result from their increased s-character.

(47) For example, CO loss from phenoxide ion is a low-energy dissociative rearrangement reaction (ΔH = 40 kcal/mol) that has a measured maximum CID cross section of only 0.3 Å^2. Moreover, CID of *o*-chlorophenoxide shows only Cl^- loss ($\Delta H \approx$ 80 kcal/mol; σ_{max} = 1 Å^2) by the kinetically-preferred direct cleavage pathway and no CO loss. Wenthold, P. G.; Squires, R. R., unpublished results.

(48) (a) Wilt, J. W. In *Free Radicals*; Kochi, J. K., Ed.; J. Wiley and Sons: New York, NY, 1973; pp 333–501. (b) Valko, L.; Simon, P. *Chem. Phys.* **1985**, *99*, 447, and references therein. (c) Li, W.-K.; Nobes, R. H.; Radom, L. *J. Mol. Struct. (THEOCHEM)* **1987**, *147*, 67.

(49) Poutsma, J. C.; Paulino, J. A.; Squires, R. R., unpublished results.

(50) Kassaee, M. Z.; Nimlos, M. R.; Downie, K. E.; Waali, E. E. *Tetrahedron* **1985**, *41*, 1579.

(51) Billups, W. E.; Chong, W. Y.; Leavell, K. H.; Lewis, E. S.; Margrave, J. L.; Sass, R. L.; Shieh, J. J.; Werness, P. G.; Wood, J. L. *J. Am. Chem. Soc.* **1973**, *95*, 7878.

(52) Dorigo, A. E.; Li, Y.; Houk, K. N. *J. Am. Chem. Soc.* **1989**, *111*, 6942.

(53) Radlick, P.; Crawford, H. J. *J. Chem. Soc., Chem. Commun.* **1974**, 127.

(54) Koga, N.; Morokuma, K. *J. Am. Chem. Soc.* **1991**, *113*, 1907.

(55) Tamagawa, K.; Iijima, T.; Kimura, M. *J. Mol. Struct.* **1976**, *30*, 243.

(56) (a) Nachtigall, P.; Jordan, K. D. *J. Am. Chem. Soc.* **1992**, *114*, 4743. (b) Nachtigall, P.; Dowd, P.; Jordan, K. D. *J. Am. Chem. Soc.* **1992**, *114*, 4747. (c) Nash, J. J.; Dowd, P.; Jordan, K. D. *J. Am. Chem. Soc.* **1992**, *114*, 10071. (d) Nachtigall, P.; Jordan, K. D. *J. Am. Chem. Soc.* **1993**, *115*, 270.

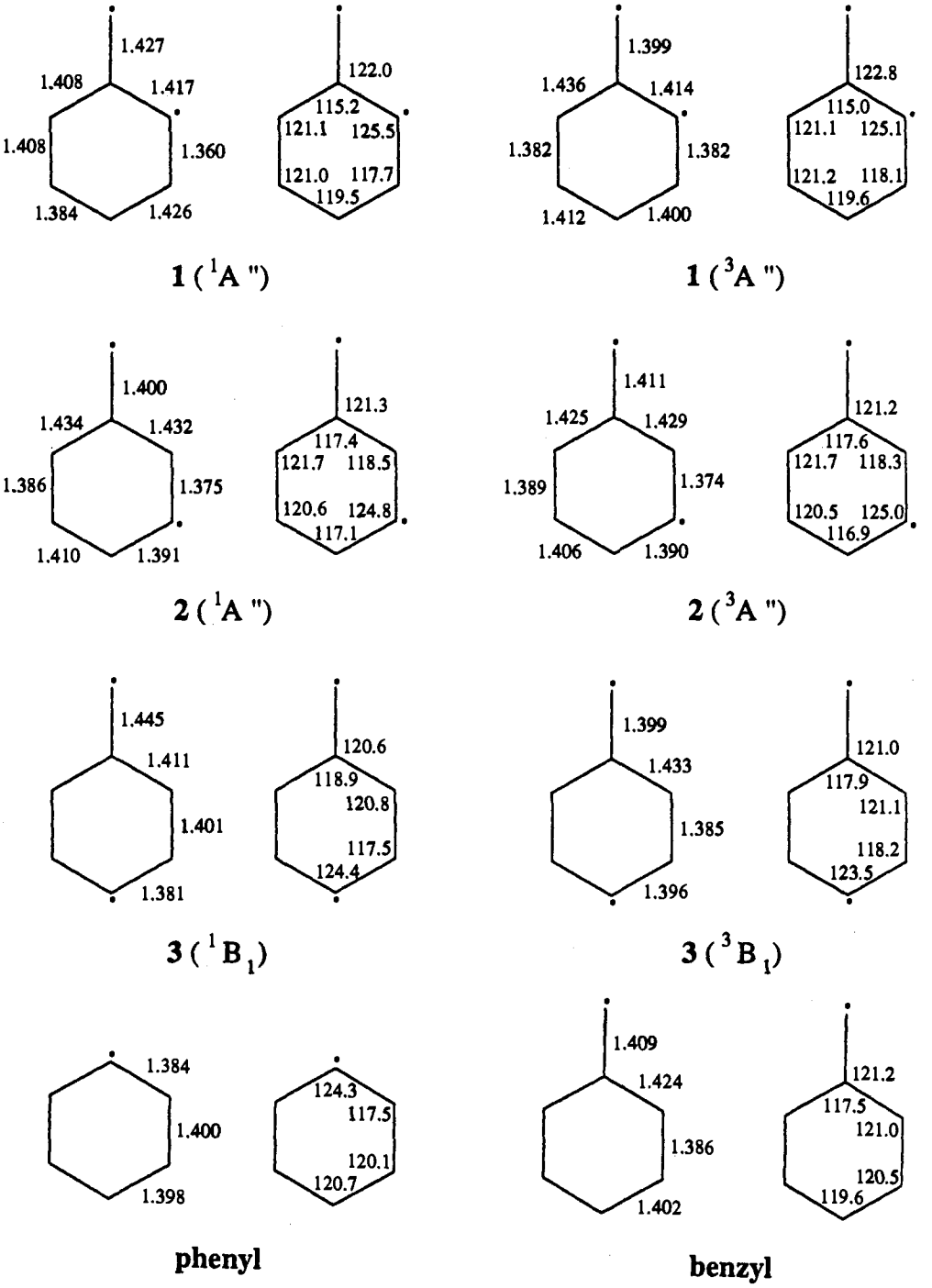

Figure 2. Calculated C–C bond lengths (Å) and CCC bond angles (deg) for the singlet and triplet states of 1–3 at the MCSCF(8,8)/3-21G level of theory.

The above structural differences are easily understood in terms of σ–π exchange interactions and how they may effect the extent of π-conjugation, the geometries, and the ground-state multiplicities of each of the biradicals. The singly-occupied, nonbonding π-molecular orbital (NBMO) of a benzylic radical is spin-polarized in the manner shown below, with the π-spin polarization at the *meta* carbons opposite to that at the C_α, *ortho*, and *para* carbons (note that the relative sizes of the π-coefficients at the nodal carbons have been enhanced for clarity[57]). High-spin coupling of the σ and π electrons at each of the dehydrocarbons will lead to a lower correlation energy,[58] giving rise to the net spin

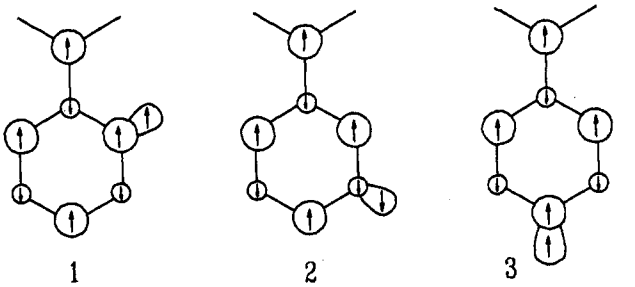

polarizations shown. On this basis, one can predict[59] triplet ground states for **1** and **3** and a singlet ground state for **2** (*vide infra*). In the triplet states for **1** and **3**, the favorable one-center exchange terms will be maximal when the π-coefficients at the dehydrocarbons are maximized. This is achieved by increasing the extent

(57) Nonzero π-coefficients at the formal "nodal" carbons of odd alternant hydrocarbons such as benzyl radical arise when electron correlation is included *via* CI or MCSCF wave functions; see: Borden, W. T. *Modern Molecular Orbital Theory for Organic Chemists*; Prentice-Hall, Inc.: Englewood Cliffs, NJ, 1975; Chapters 5 and 9.

of π-conjugation between the exocyclic carbon and the ring, i.e., by *shortening* the C_α–C_1 bond relative to benzyl radical. In contrast, the correlation energy is greater in the singlet states for **1** and **3** since the σ- and π-electrons at the dehydrocarbons are necessarily low-spin coupled. In this case, minimization of the π-coefficient at the dehydrocarbon is preferred, so π-conjugation with the exocyclic carbon is reduced by *lengthening* the C_α–C_1 bond relative to benzyl radical. Because of the much smaller size of the π-coefficient at the *meta* carbons in the benzylic π-NBMO (π_4), the magnitude of the σ–π exchange interaction at the dehydrocarbon of **2** is smaller, and the geometric distortions in the singlet and triplet states relative to benzyl radical are small. The natural orbital coefficients for the π-NBMO obtained from the MCSCF(8,8)/pVDZ calculations for **1–3** verify this simple picture. The ratios of the coefficients at the dehydrocarbon and C_α in the π-NBMO of **1**, **2**, and **3** (c_{dehyd}/c_α) are 0.21, 0.01, and 0.21 for the singlet states and 0.59, 0.01, and 0.66 for the triplet states, respectively. These may be compared to the corresponding ratios for the *ortho*, *meta*, and *para* carbons of benzyl radical, which are 0.64, 0.01, and 0.49, respectively.

The optimized geometries obtained for the closed-shell singlet states of **1–3** at the MCSCF(2,2)/6-31G* (for **1** and **3**) and RHF/6-31G* (for **2**) levels exhibit pronounced C–C bond length alternation as expected for the valence bond structures shown below.

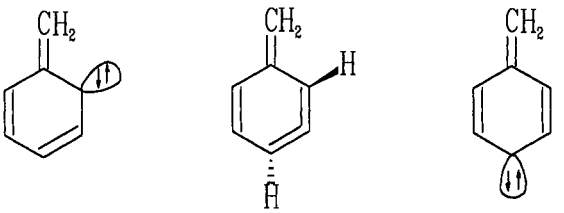

$^1A'$ 1 ^1A 2 $^1A_1$ 3

Moreover, ^1A **2** possesses a highly puckered ring as a result of the 1,2-diene moiety, similar to other cyclic cumulenes.[60] For example, the CCC bond angle about the dehydrocarbon is 132°, and the *o*- and *p*-hydrogens are bent out of their local molecular planes by about 17°, while the *m*-hydrogen and C_α are bent out of their local planes by about 11°.

Energetics. The absolute energies, singlet–triplet splittings, and predicted heats of formation based on the computed BSE values for **1–3** are listed in Table 5. Although higher level MCSCF or CI calculations were not carried out, it is clear from the MCSCF(2,2)/6-31G* and RHF/6-31G* calculations that the closed-shell singlet states of **1–3** are much higher in energy than the open-shell singlets and triplets. For **1** and **3**, the MCSCF-(2,2)/6-31G* energy difference between the closed-shell singlets and the lower energy open-shell states is 16–18 kcal/mol, while for **2** the closed-shell form is 33–34 kcal/mol higher in energy. This state ordering is expected for nonpolar, "heterosymmetric" biradicals,[61] wherein the two singly-occupied orbitals have different symmetries. Unlike methylene, where the "ionic" $^1A_1$ singlet state lies energetically below the "covalent" $^1B_1$ singlet state, the reduced one-center Coulomb repulsion ($J_{\sigma\pi}$) and electron exchange ($K_{\sigma\pi}$) between the localized σ-NBMO and the *delocalized* π-NBMO in **1–3** reduces the energy of the covalent singlet states such that they lie below the ionic singlet states.

With the exception of the MCSCF(2,2)/6-31G* results for **2**, all of the theoretical methods concur with the ground-state multiplicity predictions made from simple spin polarization arguments: **1** and **3** are ground-state triplets, and **2** is a ground-state singlet. These assignments are consistent with the available experimental data for **1–3** and their analogs. Derivatives of biradical **1** were generated in low-temperature matrices more than 25 years ago that displayed characteristic triplet ESR spectra and zero-field splitting parameters which were consistent with methylenecyclohexadienylidene character mentioned above.[5] Sander and co-workers isolated the oxo analog of **3**, α,4-dehydrophenol (4-oxo-2,5-cyclohexadienylidene) in an argon matrix and assigned a triplet ground state based on the measured ESR spectrum.[6] Myers and co-workers examined the reactivity of biradical **2** in various solvents and attributed the observed product distributions to its polar (singlet), as opposed to biradical (triplet) character.[7] Moreover, the topologically-related bent-planar allene system, which can be viewed as a 2-dehydroallyl biradical, was examined computationally by Johnson and co-workers and was found to have a (covalent) singlet biradical ground state lying 4.9 kcal/mol below the triplet.[62]

Given the correct ground-state assignments for the three biradicals, $^3A''$ for **1**, $^1A''$ for **2**, and $^3B_1$ for **3**, it is noteworthy that at each of the theoretical levels employed, the total energies computed for the ground state of each isomer are essentially the same within 1.2 mHartrees (0.75 kcal/mol), whereas the variance among the total energies for each of the first excited states is somwehat greater (*ca.* 9 mHartrees, 5.6 kcal/mol). This point will be addressed further in the context of the derived heats of formation.

As with most biradical calculations, the singlet–triplet splittings obtained for **1–3** are dependent upon the theoretical level used. With the higher level calculations, the largest splittings for **1–3** are obtained at the MCSCF(8,8)/pVTZ, MCSCF(8,8)/pVDZ, and MCSCF(8,8)/6-31G* levels, and the smallest values are obtained from the CISD and CCCI calculations. The MCSCF-(8,8) results for **3** using the pVTZ and pVDZ basis sets are the same, suggesting that the calculations have probably converged with respect to basis set size. The MCSCF(8,8)/6-31G* results for all three biradicals are comparable to the MCSCF(8,8)/pVDZ results, despite the significant differences in the geometries used for the total energy calculations. Because the pVDZ and 6-31G* basis sets are similar in size, this suggests that the singlet–triplet energy gaps are not especially sensitive to the structural details. The MCSCF(8,8), CISD, and CCCI calculations predict similar singlet–triplet splittings for **1** and **3**. The smaller singlet–triplet splitting computed for **2** at each level of theory is expected because of the smaller σ–π exchange interaction that results when the singly-occupied σ-orbital is located at a "nodal" carbon of the benzylic π-NBMO.[57]

In order to derive heats of formation for **1–3** from the total energies, the enthalpy changes for the hypothetical isodesmic reactions shown in Scheme 2 were calculated at a consistent level of theory. These "biradical separation energies" (BSE) listed in Table 5 indicate the stability of each biradical system relative to a hypothetical "noninteracting" biradical model that would be derived from a simple bond energy additivity calculation. That is, they provide a measure of the strengths of the ring C–H bonds in benzyl radical relative to benzene or, alternatively, the strength of the benzylic C–H bonds in *o*-, *m*- and *p*-tolyl radicals compared to toluene. Positive BSE values indicate that the biradical is stabilized (bonds are weaker), while negative BSE values indicate destabilization (bonds are stronger). For **1** and **3**, all of the theoretical levels employed indicate that the triplet states are stabilized and the singlet states destabilized and that the absolute magnitudes of the BSEs are larger for the singlets than for the triplets. All of the higher level calculations indicate that the ground states of the three biradicals are *stabilized* relative to the noninteracting biradical model.

(58) Salem, L. *Electrons in Chemical Reactions*, J. Wiley: New York, NY, 1982; Chapter 7.
(59) (a) Borden, W. T.; Davidson, E. R. *J. Am. Chem. Soc.* **1977**, *99*, 4587. (b) Borden, W. T. In *Diradicals*, Borden, W. T., Ed.; Wiley: New York, 1982, Chapter 1.
(60) Johnson, R. P. *Chem. Rev.* **1989**, *89*, 1111.
(61) Salem, L.; Rowland, C. *Angew. Chem., Int. Ed. Engl.* **1972**, *11*, 92.
(62) Angus, R. O., Jr.; Schmidt, M. W.; Johnson, R. P. *J. Am. Chem. Soc.* **1985**, *107*, 532.

The BSE values were combined with the experimentally-known heats of formation for benzene, phenyl radical, and benzyl radical (Table 1) in order to compute the heats of formation for each biradical. The predicted heats of formation for the singlet and triplet states of **1–3** listed in the last column of Table 5 span a range of 105–114 kcal/mol. The value derived from bond energy additivity (corresponding to BSE = 0) is 107.6 ± 1.7 kcal/mol, as calculated from eq 5 and the auxiliary thermochemical data listed in Table 1.

$$\Delta H°_{f,298}(C_6H_4CH_2) = \Delta H°_{f,298}(C_6H_5CH_3) + DH°_{298}[C_6H_5\text{–}H] + DH°_{298}[C_6H_5CH_2\text{–}H] - 2\Delta H°_{f,298}(H) \quad (5)$$

We believe that the MCSCF(8,8)/pVDZ results are the most realistic because of the better treatment of excitations involving the π*-orbitals in estimating the correlation energy. Although the CISD calculations include a total of 378 013–766 528 configurations in estimating the correlation energy for the open-shell singlet and triplet states of **1–3**,[63] the use of a single reference configuration and allowing only single and double excitations will tend to underrepresent the electron density in the π*-orbitals that is crucial for properly describing the σ–π exchange interactions at the dehydrocarbon atoms. In contrast, the MCSCF(8,8) calculations more completely represent the electron density in the π*-orbitals since *all* symmetry allowed excitations within the active space are included. The CCCI calculations, which use a contracted CI space and involve relatively small numbers of configurations (4800–5200), also may not adequately represent the electron density in the π*-orbitals since, unlike in the MCSCF-(*n*,*n*) procedures, the shapes of the reference orbitals used for the limited CI procedure are not optimized.

The MCSCF(8,8)/pVDZ calculations predict identical heats of formation for $\tilde{X}\,^3A''$ (**1**), $\tilde{X}\,^1A''$ (**2**), and $\tilde{X}\,^3B_1$(**3**) of about 105 kcal/mol, with singlet–triplet splittings (ΔE_{ST}) of –7.4, 3.0, and –8.1 kcal/mol, respectively (the MCSCF(8,8)/pVTZ results for **3** are virtually identical). The predicted heats of formation have an estimated uncertainty of about 3–4 kcal/mol, based on the range of BSE values obtained from all of the higher level calculations and the uncertainties in the experimental data used to compute them. The MCSCF(8,8)/pVDZ derived heats of formation and the measured values based on the iodobenzyl anion CID experiments (103 ± 3 kcal/mol) are within the combined uncertainties, as shown in the schematic summary provided by Figure 3. Although the agreement between experiment and theory is satisfactory, we must comment on the remaining 2 – 3 kcal/mol differences since it could be argued that the theoretical results are showing that the measured values are systematically too low. Indeed, in the earlier study of benzyne thermochemistry, theory played a critical role in exposing a chemical contamination problem in the experimental results that led to heats of formation for *m*- and *p*-benzyne that were too low by 9–10 kcal/mol.[2] However, an analogous contamination problem in the present CID experiments is not possible since the halobenzyl anions cannot isomerize to any lower energy isomers. Furthermore, the absolute accuracy of the measured heats of formation for the dehydrotoluenes is strongly supported by the following facts: (1) the *same* value is derived for α,3-dehydrotoluene from three different halobenzyl anion precursors, despite the differing ion lifetime and internal energy effects used in the three analyses and the use of completely different auxiliary thermochemical data; (2) the *same* heat of formation for **2** (104.1 ± 3.8 kcal/mol) is also derived from experimental results involving a completely different thermochemical cycle that combines CID threshold measurements

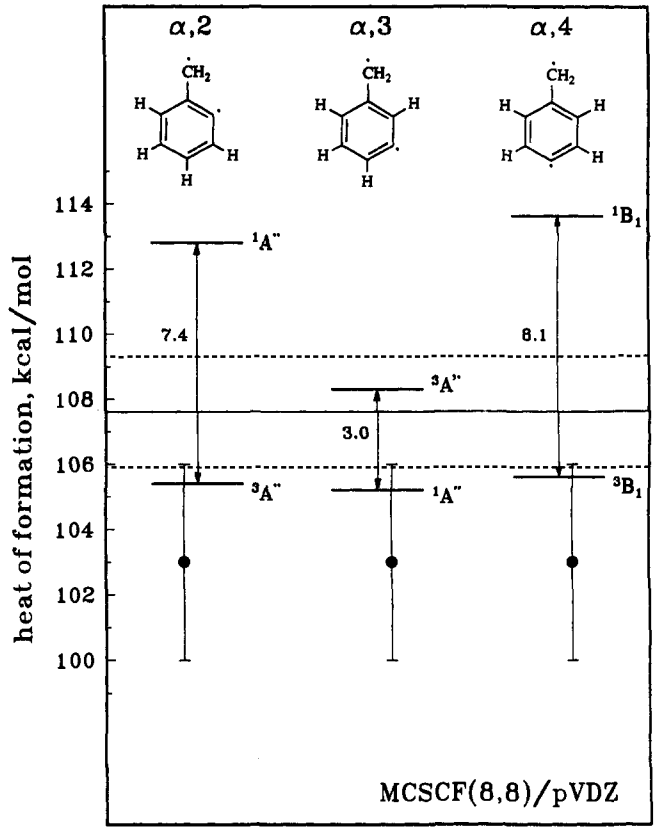

Figure 3. Calculated heats of formation for the singlet and triplet states of α,2-, α,3-, and α,4-dehydrotoluene derived from the corresponding BSE values (Scheme 2, eq 5) obtained at the MCSCF(8,8)/pVDZ//MCSCF(8,8)/3-21G level of theory. The heat of formation for a generic α,n-dehydrotoluene molecule based on bond strength additivity (107.6 ± 1.7 kcal/mol) is indicated by the solid horizontal and dashed lines, and the experimental heats of formation for each dehydrotoluene (103 ± 3 kcal/mol) are indicated with solid circles.

for cations with photoelectron measurements;[64] and (3) the absolute heats of formation for a variety of other species, including benzyl cation,[64] phenyl cation,[65] and dichlorocarbene,[1] determined by CID threshold techniques with our instrument are in excellent agreement with the recommended[31,44] literature values, thereby ruling out any systematic effects in our measurements or analyses that produce low values.

We therefore attribute the remaining 2–3 kcal/mol differences between the experimental and theoretical heats of formation for the dehydrotoluenes to a failure of the present levels of theory to account completely for the σ–π correlation energies in these systems that are so crucial in determining the absolute and relative energies of the open-shell singlet and triplet states. A multi-reference CI approach including triple excitations is probably necessary to achieve a proper description of the electronic structures and energetics of these biradicals.

The experimental and theoretical results summarized in Figure 3 reveal some unexpected features in the relative and absolute energetics of the dehydrotoluene biradicals. First, the singlet and triplet states of **1** and **3** are unsymmetrically distributed about the noninteracting biradical (bond additivity) energy level, i.e., the singlet states appear to be destabilized by about 3 times as much as the triplets are stabilized. A simple two-orbital, two-electron model for heterosymmetric, ground-state triplet biradicals would predict equal and opposite splitting of these energy levels by the σ–π exchange energy, $K_{\sigma\pi}$.[66] A more detailed analysis of the exchange interactions at the ROHF (MCSCF(2,2)) level of

(63) The MOLPRO program uses a contracted-CI algorithm. The number of uncontracted configurations ranged from 681 665 to 2 823 790.

(64) Chen, P.; Logan, C. F.; Ma, J. C; Wenthold, P. G.; Squires, R. R., manuscript in preparation.

(65) Wenthold, P. G.; Squires, R. R., unpublished results.

theory provides a partial explanation for the unsymmetrical splitting of the singlet and triplet states of **1** and **3**.[67] In triplet **3** there are 4/7 π-electron at the dehydrocarbon with the same spin as the σ-electron, giving a net contribution to the exchange energy of $(-4/7)K_{\sigma\pi}$. For singlet **3**, there are 3/7 π-electron at the dehydrocarbon with the same spin as the σ-electron, giving $(-3/7)K_{\sigma\pi}$ contribution to the exchange energy, to which one must add $(1/7)K_{\sigma\pi}$ to account for the destabilizing exchange interaction between the two open-shell electrons with opposite spin. Therefore, the net exchange energy contribution to the total energy of singlet **3** is $(-2/7)K_{\sigma\pi}$. These same values would be derived for singlet and triplet **1**. At the ROHF (MCSCF-(2,2)) level of theory, the singlet and triplet states of **2** are essentially degenerate and have BSE values near zero, so the exchange energy contribution in **2** can serve as a "noninteracting biradical" reference value for **1** and **3**. In biradical **2**, half the π-electrons at the dehydrocarbon have the same spin as the σ-electron, giving a net exchange energy contribution of $(-1/2)K_{\sigma\pi}$ to the total energy. Therefore, triplet **3** should be only $(-4/7)K_{\sigma\pi} - (-1/2)K_{\sigma\pi} = (-1/14)K_{\sigma\pi}$ more stable than **2**, but singlet **3** should be $(-2/7)K_{\sigma\pi} - (-1/2)K_{\sigma\pi} = (3/14)K_{\sigma\pi}$ less stable than **2**. That is, compared to biradical **2** as a model for a dehydrotoluene with no open-shell π-electron density at the dehydrocarbon, the singlet states of **1** and **3** are destabilized by 3 times as much as the triplet states are stabilized at the ROHF level of theory. Geometry differences between the singlet and triplet states and differential correlation effects will further influence the splitting; however, the MCSCF and CI results suggest that these effects are small.

Second, one would not have predicted *a priori* that all three biradical ground states should have the same heat of formation that is 4–5 kcal/mol below the bond additivity estimate. For **1** and **3** this is understandable because of the σ–π exchange interaction in the ground-state triplets that is ignored in the bond additivity model. The exchange energy for the prototype 1,1 σ–π biradical CH_2 is about 15 kcal/mol ($(1/2)\Delta E$ for the $\tilde{X}\,^3B_1$ and $\tilde{b}\,^1B_1$ states[68]), so a value of 4–5 kcal/mol for a biradical with a delocalized π-system seems reasonable. For **2** the exchange interaction in the triplet state is much smaller than that in **1** and **3** because of the much smaller π-coefficient at the dehydrocarbon, and, accordingly, the energy of the triplet is nearly equal to the bond additivity estimate. As a result, the absolute heat of formation for ground-state singlet **2** can be reasonably well approximated from simple valence promotion energy models,[69] i.e., by the difference between the bond energy additivity estimate and the singlet–triplet gap. However, this does not explain *why* singlet **2** is stabilized to such an extent that it becomes degenerate with triplet **1** and triplet **3**. Geometrical factors are not responsible, since the MCSCF(8,8)/pVDZ energies of the three biradical ground states all increase by the same amount (*ca.* 1 kcal/mol) when their geometries are constrained to that of benzyl radical. The weighting coefficients of the configuration state functions associated with the MCSCF(8,8)/pVDZ wave functions provide some important clues. These indicate distinctly *greater* contributions from configurations derived from $\pi \rightarrow \pi^*$ excitations involving the two highest-lying doubly-occupied π-orbitals (π_2 and π_3) and the two lowest-lying virtual π-orbitals (π_5 and π_6)

(66) This zeroth-order model is valid only if the geometries of the singlet and triplet states are identical, a requirement that is not fulfilled by **1** and **3** (cf. Table 4 and Figure 2). However, test calculations of the total energies of the singlet and triplet states of **1** and **3** held at the geometry of benzyl radical show the same basic trend: the singlet states are destabilized by roughly 3 times as much as the triplet states are stabilized.

(67) We reproduce here the insightful analysis provided by Professor Wes Borden (personal communication). We are grateful to Professor Borden for bringing this model to our attention.

(68) Herzberg, G. *Molecular Spectra and Molecular Structure III. Electronic Spectra and Electronic Structure of Polyatomic Molecules*; Van Nostrand Reinhold: New York, NY; 1966.

(69) (a) Carter, E. A.; Goddard, W. A. III. *J. Phys. Chem.* **1986**, *90*, 998. (b) Wu, C. J., Carter, E. A. *J. Am. Chem. Soc.* **1990**, *112*, 5893. (c) Zhang, X.; Chen, P. *J. Am. Chem. Soc.* **1992**, *114*, 3147.

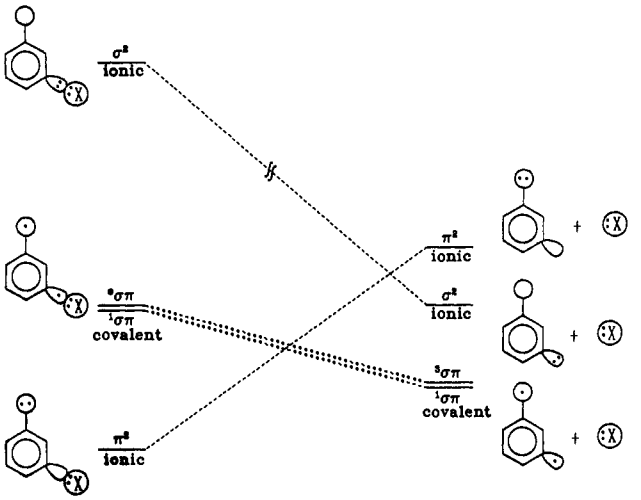

Figure 4. Schematic state correlation diagram for dissociation of a *m*-halobenzyl anion with a C_s (planar) symmetry constraint.

in singlet **2** compared to triplet **2** or any of the other biradicals (singlet or triplet). These are precisely the $\pi \rightarrow \pi^*$ excitations that are necessary in order to increase negative spin density at the *meta* dehydrocarbon in singlet **2**, thereby maximizing the σ–π exchange interaction at this site.

Dissociation Dynamics. Given the satisfactory agreement between theory and experiment on the thermochemistry, plus the assignments of the biradical ground-state multiplicities made above, we can now understand the origins of the halide ion dependence of the experimental results for **1** and **3**, but not for **2**. First, it may be noted that halide ion elimination from a halobenzyl anion is formally symmetry-"forbidden" for strictly planar departure of the X^- leaving group.[4] As illustrated in the state correlation diagram shown in Figure 4, this could give rise to a symmetry barrier for dissociation that, in turn, could lead to a reverse activation energy and a measured dissociation energy in excess of the thermochemical limit. However, symmetry-breaking is easily achieved by out-of-plane bending of the carbon–halide bond—a low frequency mode (25–150 cm^{-1}) that is undoubtedly highly excited in the dissociation transition states. Any other a″ vibrational excitations (b_1 for *p*-halobenzyl anions) would have the same effect. The resulting σ,π mixing relaxes the symmetry barrier and ultimately makes the dissociations "allowed".[4] Accordingly, a plausible explanation for the halide ion dependence of the apparent heats of formation for **1** and **3** might be that the successively decreasing out-of-plane bending potentials for the heavier halides lead to successively decreasing symmetry barriers and, thus, smaller reverse activation energies and lower apparent heats of formation. However, the absence of any halide ion dependence of the results for **2**, despite the presence of the same formal symmetry constraints, argues against this explanation. Given that nonplanar pathways will constitute nearly all of the available phase space for halobenzyl anion dissociations, these formal symmetry barriers are probably of little or no consequence in the CID threshold measurements.

The more likely explanation for the differing behavior of the halobenzyl anions involves the effects of the biradical spin states on the dissociation energetics and dynamics. The dissociations of *o*- and *p*-halobenzyl anions to ground-state triplet biradicals are spin-forbidden reactions and, therefore, necessarily involve a curve-crossing mechanism. Schematic potential energy surfaces for this type of reaction are depicted in Figure 5. Key considerations are the actual location of the crossing between the singlet and triplet diabatic surfaces relative to the energy of the triplet biradical + X^- products and the extent of configuration mixing at this point, since these factors will determine the activation energy for halide ion loss that is measured in the CID threshold experiment. Note that although the triplet biradical–

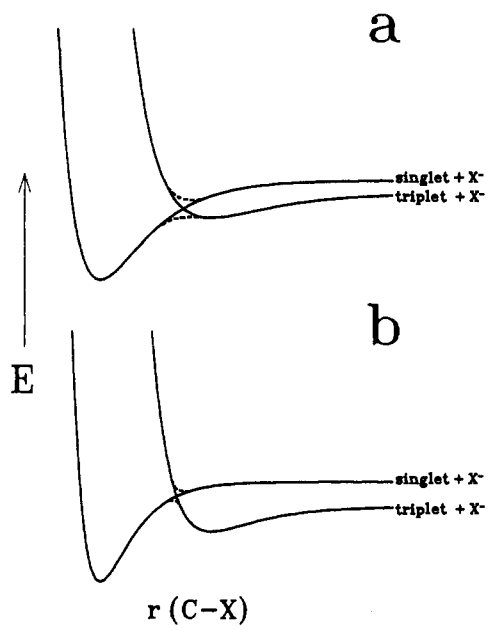

Figure 5. Schematic potential energy surfaces involved in dissociation of halobenzyl anions to dehydrotoluene biradicals with triplet ground states: (a) surface crossing occurs at an energy below the triplet asymptote, (b) surface crossing occurs at an energy above the triplet asymptote.

halide ion interaction is highly repulsive at normal bonding distances, it is slightly attractive at longer distances due to electrostatic (ion–dipole and ion-induced dipole) interactions. Thus, the triplet surfaces will have shallow minima at different distances and with different well depths for each different halide ion. Figure 5a illustrates a situation where the crossing occurs at energies below the triplet product asymptote. In this case, the measured CID threshold energy will be equal to the reaction endothermicity (*vide infra*). However, if the surface crossing occurs on the steeply-rising, repulsive portion of the triplet surface, then the situation illustrated in Figure 5b results. This would give rise to a reverse activation energy for the dissociation and a CID threshold energy that exceeds the reaction endothermicity by an amount approaching the singlet–triplet energy difference for the biradical.

It is not known *a priori* where the singlet–triplet surface crossings occur nor which situation illustrated in Figure 5 best describes *o*- and *p*-halobenzyl anion dissociations. However, if Figure 5b pertains, then the halide ion dependence of the results can be rationalized as follows. In going from Cl^- to Br^- to I^-, the minima in both the singlet and triplet surfaces shown in Figure 5b will become shallower and will occur at longer distances, but the changes will be more pronounced with the singlet surface than with the triplet surface due to the stronger (covalent) nature of the halide ion binding in the former. The net effect will be a natural decrease in the reverse activation energies for the dissociations involving the heavier halides, perhaps to such an extent that the situation shown in Figure 5a is achieved for X = I. For these same reasons, both potential energy surfaces in the vicinity of the curve crossing will become less precipitous with the heavier halides, i.e., the slopes of the two diabatic surfaces will decrease, as will their difference. This would lead to an increase in the efficiency of intersystem crossing in accordance with the Landau–Zener model for electronically nonadiabatic processes[70] (eq 6), where $P_{S\to T}$ is the probability for singlet-to-

$$P_{S\to T} = 1 - \exp\left(-\frac{4\pi V_{ST}^2}{h\nu|m_S - m_T|}\right) \qquad (6)$$

triplet conversion during dissociation, V_{ST} is one-half the splitting between the potential energy surfaces at the crossing, ν is the velocity of the system at the crossing (e.g., the rate of change of the carbon–halide bond distance), and $|m_S - m_T|$ is the difference in the slopes of the unmixed diabatic surfaces at the crossing. Thus, the intersystem crossing probability rapidly approaches unity as the surface energy gradients decrease, as the system spends more time near the crossing (ν decreases), or as the configuration mixing increases.

The above discussion assumes that dissociation of the *o*- and *p*-halobenzyl anions occurs at the statistical rates, i.e., that adiabatic dissociation occurs at rates limited only by the activated ion lifetimes that are adequately modeled by RRKM theory.[16] However, it is certainly possible for the singlet–triplet intersystem crossing in these species to be slow on the experimental time scale (*ca.* 30 μs), an effect that could give rise to an additional kinetic shift in the observed dissociation onsets not accounted for by the RRKM analysis. In view of the fact that transitions between the triplet and open-shell singlet states of **1** and **3** are formally spin–orbit-forbidden,[61] this may in fact be a likely explanation for the observed halide ion dependences. That is, as the carbon–halide bond begins to stretch in the activated ion (and bend out of the molecular plane), open-shell singlet biradical character evolves as the system procedes along the singlet surface (cf. Figure 4). The greater the open-shell singlet character at the nominal curve-crossing, the slower will be the rate of intersystem crossing since the singlet–triplet electronic transition does not involve a change in orbital angular momentum.[61] In the limit where no intersystem crossing occurs, the measured threshold would correspond to the formation of the open-shell singlet biradical. However, the rate of intersystem crossing would be expected to increase in the presence of the heavier halides (Br^-, I^-) due to heavy atom induced spin–orbit coupling,[4a] and, as a result, the kinetic shifts would disappear. It is noteworthy in this regard that the apparent heats of formation obtained for **1** and **3** from the chlorobenzyl anion results are higher than the iodobenzyl anion derived values by amounts that are nearly the same as the predicted singlet–triplet splittings (7–8 kcal/mol). This suggests that the *o*- and *p*-chlorobenzyl anions dissociate diabatically. Model calculations indicate that intersystem crossing in the activated chlorobenzyl anions would need to have an efficiency of *ca.* 0.3% to account for this behavior.[71] Thus, the halide ion dependence of the results for **1** and **3** could be a manifestation of heavy atom effects on the rates of unimolecular decomposition involving spin–orbit-forbidden transitions.

Either or both of the above effects could account for the results obtained from the *o*- and *p*-halobenzyl anions. In contrast, because α,3-dehydrotoluene has a singlet ground state, dissociation of a *m*-halobenzyl anion is *spin-allowed* and thus can occur on a single diabatic potential energy surface. Therefore, these dissociations take place at the true thermochemical limit regardless of the halide ion leaving group. Indeed, the absence of a halide effect on the apparent heat of formation for α,3-dehydrotoluene provides indirect proof that it possesses a singlet ground state.

Related Thermochemical Properties. The experimentally determined heats of formation for **1**–**3** can be used in conjunction with other data from the literature to derive additional thermochemical properties for related species. First, it is evident from the discussion concerning BSEs that the ring C–H bonds in benzyl radical are significantly weaker than the benzene C–H bond ($DH_{298}[C_6H_5$–H] = 111.2 ± 0.8 kcal/mol[41]); a common value of 107 ± 3 kcal/mol is derived for the *ortho*, *meta*, and *para* C–H bond strengths in benzyl radical from the biradical heats of formation. Similarly, *o*-, *m*-, and *p*-tolyl radicals have benzylic C–H bond strengths about 4–5 kcal/mol less than that for toluene ($DH_{298}[C_6H_5CH_2$–H] = 88.5 ± 1.5 kcal/mol[44]), or about 84 ± 3 kcal/mol. Similar effects may appear in isoelectronic species.

(70) Steinfeld, J. I; Francisco, J. S.; Hase, W. L. *Chemical Kinetics and Dynamics*, Prentice-Hall: Englewood Cliffs, NJ, 1989, p 274 and references therein.

(71) This estimate is based on the assumption that the intersystem crossing would occur at the same approximate location as the dynamical bottleneck.

For example, lone-pair ionization of the picolines (methylpyridines) should weaken their benzylic C–H bonds. Similarly, ionized anilines should have weakened ring C–H bonds.

Bracketing experiments involving deprotonation of hydrogen-bearing carbocations has been used as a means to estimate heats of formation for carbenes.[72] Using $\Delta H^{\circ}_{f,298}$(benzyl cation) = 217.5 ± 1.0 kcal/mol[73] and a heat of formation for phenyl carbene of 106 ± 3 kcal/mol determined in this laboratory,[49] the proton affinities at the ring- and α-positions of a dehydrotoluene biradical are calculated to be 251 and 254 kcal/mol, respectively. Thus, benzyl cation is slightly more acidic at its ring positions than at the α-position. However, this would require an ion beam experiment to verify, since even the strongest (volatile) neutral bases known, such as the tertiary amines (PA = 230–235 kcal/mol[31]) or the α,ω-diamines (PA = 235–240 kcal/mol[31]), could not deprotonate benzyl cation under thermal conditions in the gas phase.

The energetics of certain biradical-forming rearrangements can also be derived from the dehydrotoluene thermochemistry. For example, the enthalpy of ring-opening of benzocyclopropene (ΔH_f = 89 ± 1 kcal/mol[51]) to **1** (eq 7a) can be determined to be 14 ± 3 kcal/mol. This is a remarkably low energy for an aryl/

(7a)

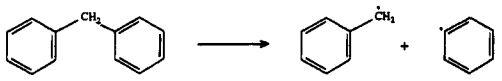

(7b)

benzylic C–C bond cleavage, considering that the analogous acyclic bond cleavage shown in eq 7b has an enthalpy change of 95 kcal/mol. The large difference is a reflection of both the strain energy in benzocyclopropene and the special stabilization of the α,2-dehydrotoluene biradical relative to benzyl and phenyl radical. From the reported activation energy for ring-opening of a substituted benzocyclopropene of 25 kcal/mol,[74] the transition state can be roughly located about 10 kcal/mol above the α,2-dehydrotoluene biradical. The relatively small energy difference suggests that the extent of CCC angle bending and CH_2 twisting relative to **1** is not large, consistent with the late transition state expected for this mildly endothermic ring-opening reaction. Similarly, Myers and co-workers have determined the activation enthalpy for formation of **2** from (*Z*)-1,2,4-heptatrien-6-yne in benzene to be 21.8 ± 0.5 kcal/mol (eq 8).[7] The overall enthalpy

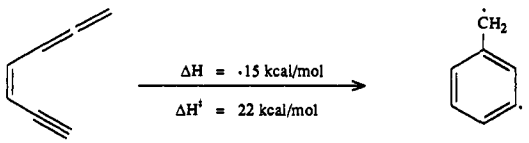

(8)

change for the reaction in the gas phase is determined from the present data and ΔH_f((*Z*)-1,2,4-heptatrien-6-yne) = 118 ± 2 kcal/mol[32] to be −15 ± 4 kcal/mol. A similar value for the reaction in benzene is expected because of the nonpolar nature of the reactants and products. Therefore, the activation energy for ring-opening of α,3-dehydrotoluene to the enyne is 37 kcal/mol.

(72) Lias, S. G.; Karpas, Z.; Liebman, J. F. *J. Am. Chem. Soc.* **1985**, *107*, 6089 and references therein.
(73) Eiden, G. C.; Weisshaar, J. C. *J. Phys. Chem.* **1991**, *95*, 6194.
(74) E_a for ring-opening of α-carbomethoxybenzocyclopropene: Closs, G. L. *Adv. Alicycl. Chem.* **1966**, *1*, 53.

Concluding Remarks

This investigation of the energy-resolved, collsion-induced dissociation of isomeric halobenzyl anions has provided several new insights regarding the energetics and dynamics of biradical-forming α,ω-elimination reactions. At the very least, it is clear that future studies of biradical thermochemistry derived from CID threshold energies involving halocarbanions will require measurements with different halides. The presence or absence of significant variations in the apparent heats of formation for the biradical products with changes in the halide ion used for the CID measurements can indicate the nature of the biradical ground states. In this study we have found that the halide dependence correlates with spin-forbidden dissociation to triplet ground-state products (**1** and **3**), while halide-independent heats of formation resulted from spin-allowed dissociations to a ground-state singlet biradical (**2**). Moreover, the differences in the apparent heats of formation for **1** and **3** derived from the X = Cl and X = I results could be interpreted as lower limits for the singlet–triplet energy gaps in these biradicals. The generality of these observations remains to be seen; it can be tested with further measurements involving both α- and α,ω-elimination reactions that produce carbenes and biradicals known to have triplet ground states.

The theoretically-predicted heats of formation for the α,*n*-dehydrotoluenes based on MCSCF calculations and the measured values derived from the iodobenzyl anion CID results are in good agreement (Figure 3), although we believe that the present calculations have not completely accounted for all of the correlation energy in the biradicals. The ground states of the three biradicals are stabilized relative to a "noninteracting" biradical model by 4–5 kcal/mol, an effect that can be ascribed to stabilizing σ,π-electron exchange interactions involving the two singly-occupied, nonbonding orbitals in the α,2- and α,4-isomers. We have acquired similar results with the topologically-related α,*n*-dehydrophenols, which suggests that this may be a general pattern in the thermochemistry of this class of biradical.[65]

Acknowledgment. We thank Professors Wes Borden, Josef Michl, and Emily Carter for many illuminating discussions on this subject. This work was supported by the National Science Foundation and the Department of Energy, Office of Basic Energy Sciences. P.G.W. is grateful to The Department of Education, Phillips Petroleum and Lubrizol for fellowships. The Pittsburgh Supercomputing Center is also acknowledged for the allocation of time on the Cray C90.

Supplementary Material Available: Optimized geometries obtained at the MCSCF(2,2)/6-31G* and MCSCF(8,8)/3-21G levels of theory for the singlet and triplet states of **1–3** and at the ROHF/6-31G* and MCSCF(7,7)/3-21G level for benzyl radical are available in GAUSSIAN 92 Z-matrix format; harmonic vibrational frequencies obtained at the MCSCF(2,2)/6-31G* level for the singlet and triplet states of **1–3** and at the ROHF/6-31G* level for benzyl radical are also available (21 pages). This material is contained in many libraries on microfiche, immediately follows this article in the microfilm version of the journal, and can be ordered from the ACS; see any current masthead page for ordering information.